590939
P53

TITLE: **EVALUATION OF THE EFFECT OF WATER VAPOR ON THE PERFORMANCE OF NASA'S NMRO CATALYSTS FOR CARBON MONOXIDE OXIDATION**

GRANT NUMBER: NAG-1-2223

PRINCIPAL INVESTIGATORS: Ates Akyurtlu
Jale F. Akyurtlu

INSTITUTION: Hampton University
Department of Chemical Engineering
Hampton, Virginia 23668

SUPPORTED BY: NASA Langley Research Center
Office of Education
Hampton, VA 23665

TECHNICAL MONITOR: David Schryer, Jeff Jordan

STUDENT RESEARCHERS: Vaughnery Ammons, Taikelia Battle, Amy Gay, Kyle Bray, Boe Washington

FINAL REPORT

Summary of Research

August 1, 1999 - March 31, 2002

TABLE OF CONTENTS

INTRODUCTION

The Noble Metal Reducible Oxide (NMRO) catalysts for the low temperature oxidation of carbon monoxide were developed by NASA for the reoxidation of carbon monoxide which forms by the dissociation of carbon dioxide during the operation of sealed carbon dioxide lasers. The NMRO catalyst, which consists of a noble metal in conjunction with a reducible metal oxide, was evaluated under conditions that will be encountered in a CO_2 laser operation, namely temperatures in the range 298 to 373 K and no significant reaction gas components other than CO, CO_2, and O_2. The NMRO catalysts may have significant potential for spin-off applications such as the prevention of carbon monoxide build-up in closed spaces as in space vehicle cabins or submarines, and the elimination of the cold start-up problem of automobile exhaust catalysts. The most significant difference in the conditions of these possible future applications is the high moisture content of the gases to be processed. Lack of understanding of the effects of water vapor and high temperature on catalyst activity and operation for extended periods are currently the main stumbling blocks for the transfer of this NASA technology to be used for commercial purposes.

In the original proposal the following objectives were stated: To obtain experimental data on the adsorption, desorption and reaction characteristics of CO and O_2 on the catalysts under high moisture conditions; to collect evidence on the presence of carbonate and hydroxyl surface species and their involvement in the CO oxidation mechanism; and to model the reaction system using a Monte-Carlo simulation to gain insight on the various steps involved. After the work has commenced the NASA technical monitor Mr David Schryer informed us that there was increased interest in the possible use of the NMRO catalysts as automobile exhaust catalysts and therefore NASA wanted to know whether the catalysts can operate at high temperatures as well as with high moisture gases. At that meeting it was decided that investigation of the high temperature performance of the NMRO catalysts should be given priority and replace the Monte-Carlo simulation objective. As a result, the modified objectives of the investigation were taken as the investigation of the high-temperature activity of the NMRO catalysts, and the effect of water vapor on the performance of these catalysts .

Background Information

The noble metal reducible oxide (NMRO) catalysts have very important applications mostly involving oxidation or reduction reactions where transfer of oxygen atoms takes place. These catalysts exhibit a strong synergy between the two metal components producing significantly higher catalytic activities compared to the single metal catalysts. This synergy may arise from three different types of interactions[1]. The presence of one component may alter the properties of the other, the two components may independently catalyze different catalytic reaction steps, and/or the two components may combine to form a different surface species that may create new catalytic sites.

The NMRO catalysts that are of interest for low temperature CO oxidation are based on either platinum or gold as noble metal. Platinum is generally associated with SnO_2 as the reducible oxide for operation below 373 K as in CO reoxidation catalyst in sealed CO_2 lasers, and with ceria or titania for higher temperature service such as automobile exhaust applications. With Au, the highest activities were obtained when titanium and manganese oxides were used as the reducible oxides.

Pt/SnO_2-based catalysts were extensively studied for CO_2 laser applications by NASA/LaRC researchers and investigators in associated universities[2,3,4,5,6,7,8]. These studies have led to the optimization of the Pt/SnO_2-based catalysts with 15-20 % Pt and 5% Pd pretreated at 398 K under

reducing conditions. There is evidence that surface OH groups participate in the oxidation of CO chemisorbed on Pt sites. In fact, humidification of the catalyst surface after pretreatment or humidification of the reaction gas mixture, was reported to increase catalyst activity. The Pt/SnO_2 catalyst exhibited both long-term and short-term deactivation. Outgassing the CO_2 could restore catalyst activity after short-term decay, and the long-term deactivation could be reversed by the reduction of the catalyst. Isotopic studies have revealed the formation of some carbonate and bicarbonate species on the surface probably contributing to the short-term activity decay. About 15 % of the CO_2 was formed by the reaction of adsorbed CO with a lattice oxygen from the tin oxide situated adjacent to the noble metal and the rest resulted from the reaction of CO adsorbed on Pt reacting with the dissociatively adsorbed oxygen at the $Pt-SnO_2$ interface. Due to the strength of the O_2 double bond, direct reaction of adsorbed CO and oxygen on the catalyst surface is not probable. Instead, Schryer and Upchurch[9] propose two possible mechanisms involving surface hydroxyl groups. One mechanism involves oxidation of chemisorbed CO by OH to form CO_2 and hydrogen. The CO_2 desorbs to form gas phase carbon dioxide while the OH is regenerated by the reaction of hydrogen with the chemisorbed oxygen. The second mechanism is supported by the DRIFTS data and involves the chemisorption of CO on Pt sites while oxygen is chemisorbed on hydroxylated Sn sites through six hydroxyl groups. This type of chemisorption weakens the O_2 double bond thus allowing for the reaction of oxygen with the adsorbed CO on a neighboring Pt site.

Haruta, et. al.[10] reported high catalytic activity for CO oxidation on gold supported on TiO_2, α-Fe_2O_3, Co_3O_4, NiO, $Be(OH)_2$, and $Mg(OH)_2$ even at temperatures below 273 K. Their results were taken as an indication of the involvement of adsorbed oxygen in the chemisorption of CO. Their proposed reaction mechanism involved the formation of bidentate carbonate species by the reaction of CO adsorbed on gold and activated oxygen formed on the support at the gold-support interface.

Gardner, et. al[11] synthesized and tested several alternative low temperature CO oxidation catalysts mostly based on manganese oxide as the reducible oxide. They have observed that Au/MnO_x catalyst exhibited significantly higher activity than that of the optimized Pt/SnO_2 catalyst and almost no deactivation. The Au/MnO_x catalyst was cheaper and required no pretreatment. However, Au/MnO_x is deactivated by high concentrations of CO_2 and therefore, Au/MnO_x is less useful than Pt/SnO_2 in closed CO_2 lasers and the treatment of combustion gases.

In contrast to the involvement of surface hydroxyl groups in CO oxidation on Pt/SnO_2 catalysts, measurements on Pt/CeO_2 catalysts do not indicate the involvement of hydroxyl groups. Jin, et.al.[12] concluded that the lattice oxygen at the $Pt-CeO_2$ interface was involved in the formation of CO_2 from CO and the formation of CO from CO_2 occurred through the donation of oxygen from CO_2 to a lattice vacancy. Pre-dosing of water before the CO-TPD indicated adsorption of water but did not change the CO and CO_2 desorption profiles indicating that surface water did not take part in the formation of CO and CO_2. The CO-TPR results of Martinez-Arias, et. al.[13] also do not indicate any involvement of surface water or hydroxyl groups below 550 K on $Pt/CeO_2/Al_2O_3$. They attributed the enhanced activity at low temperatures to the enhancement of the reducibility of both the Pt and the ceria in close vicinity of the Pt-Ceria interface.

EXPERIMENTAL

For the temperature programmed reduction (TPR), Temperature Programmed Oxidation (TPO), and Temperature Programmed Reaction (TPRn) experiments Micromeritics Pulse Chemisorb 2705 apparatus with TPD/TPR 027 option was used in conjunction with a Varian 3800 Gas Chromatograph (GC)-

Saturn 2000 Mass Spectrometer (MS) for the analysis of the gaseous products. Gas mixtures used for these purposes were 6.69% H_2 in Ar, 3.6% O_2 in He, and 10.1 % CO in He. Water vapor was introduced by bubbling the feed gas stream through water at room temperature (20-25°C). To allow for better estimation of the extent of reduction a 3 °C/min heating rate was used for the TPR runs while a 5°C/min heating rate was used in TPO experiments to reduce the run time.

TPD experiments were performed by injecting 0.993-ml doses of 10.1% CO in He into the test cell until the observed peak areas remained constant. Helium was used as the carrier gas. Subsequently, the temperature of the test cell was increased at a rate of 5°C/min to obtain the desorption peaks.

A cold trap containing propanol slush, prepared by mixing propanol with liquid nitrogen, was used during TPR runs with hydrogen and for all runs with wet gases.

RESULTS

The investigation consisted of two main sections. Since the activity of the tin oxide-based oxidation catalysts will depend on their reduction-oxidation behavior under the conditions of the proposed commercial applications, the first part of the investigation focused on the TPR of the fresh and re-oxidized baseline 15% Pt/SnO_2 catalyst up to 1000 °C and under wet or dry reduction/oxidation conditions, and the TPR of some modified tin oxide based catalysts. The second part involved a series of TPD and TPRn studies aimed at obtaining information on the mechanism of CO oxidation. The results that were obtained can be classified into four groups: TPR results that show the effect of water vapor on the reduction-oxidation ability of the 15% Pt/SnO_2 catalyst, TPR results for various different catalysts prepared by NASA Langley Research Center (NASA/LaRC), TPD results to show the effect of various pre-treatments, and results of the TPRn studies combined with gas analysis using a gas chromatograph-mass spectrometer system.

Effect of Water on the Reduction-Oxidation Properties of the 15%Pt/SnO_2 Catalyst

Three sets of TPR-TPO runs were made to find out if the reduction and re-oxidation of the catalyst was affected by the presence of water.

Figures 1-3 show the results for dry reduction, dry re-oxidation, and dry reduction of the re-oxidized catalyst. Two distinct reduction peaks, one at around 130 °C and the other at around 425 °C are observed for the fresh catalyst (Figure 1). The small jump in the TCD signal just above 500 °C is probably due to the flow disturbance introduced by the addition of liquid nitrogen to the cold trap to re-freeze the propanol. The addition of liquid nitrogen to the trap always produced severe fluctuations in the TCD signal, which in most cases returned to normal. Occasionally, the condensed moisture froze and partially or totally blocked the flow path, which resulted in permanent flow disturbance until the cold trap is heated to restore the flow. To illustrate this, the points of liquid nitrogen additions and total flow path blockage are shown on some of the TPR curves. Dry re-oxidation of the reduced catalyst is seen to be slow, with a rate proportional to the temperature indicating mass transfer control of this process (Figure 2). The TPR of the re-oxidized catalyst exhibits two distinct reduction regions, a wide peak around 350 °C, and an incomplete high temperature peak, which starts at around 750 °C. The shape of the low-temperature peak also suggests mass transfer limitation at temperatures below 300 °C. Figures 4 and 5 show the amount of hydrogen consumption by the fresh and re-oxidized catalysts. From these graphs it can be observed that the oxidation-reduction capacity of the catalyst has decreased significantly when the catalyst was subjected to dry TPR up to about 1000 ° C. This may be due to the loss of OH groups that were

attached to tin oxide, but since Figures 2 and 3 indicate the presence of mass transfer limitations, the deterioration of the low temperature reduction-oxidation activity may be, at least partially, due to the loss of active sites due to sintering at the high temperatures involved.

Figures 6-8 show the results for dry reduction, wet re-oxidation, and dry reduction of the re-oxidized catalyst. Figure 6 shows the results of a TPR under the same conditions of those of Figure 1 and gives an indication of the reproducibility of the results. Comparison of Figure 7 with Figure 2 shows a higher oxidation rate during wet oxidation, which starts after 500 °C with a peak at around 725 °C. The higher oxidation rate is also confirmed by the larger reduction peaks that were obtained during subsequent dry reduction (Figure 8) compared to those shown in Figure 3. A more quantitative indication of the reproducibility of the results can be obtained by comparing the hydrogen consumption figures shown in Figures 4 and 9. Reproducibility of the total hydrogen consumption is quite good (8.18 ml STP H_2 versus 8.25 ml). The slight discrepancy (1.87 ml STP versus 1.29 ml) in the amounts of hydrogen consumption corresponding to the low temperature reduction peak is mainly due to the placement of the baseline, which is complicated by the disturbances introduced during the addition of liquid nitrogen to the cold trap as discussed above. In order to obtain a more reasonable quantitative result, the flow disturbance seen in Figure 8 is omitted in Figure 10 and the results are reported as estimates. Figure 10 shows that the low temperature reduction peak after wet re-oxidation is about 2.5 times larger than the low temperature reduction peak obtained after dry re-oxidation. It is also observed that a more significant increase in the high temperature reduction is obtained following wet re-oxidation.

Figures 11-13 present the results for the wet reduction, dry re-oxidation, and wet reduction of the re-oxidized catalyst and Figures 14 and 15 provides quantitative results for the wet reduction of the fresh and dry re-oxidized catalyst. Figures 16-20 present the corresponding results for the case of wet reduction, wet re-oxidation, and wet reduction. Comparison of Figures 11 and 16 with Figures 1 and 6 show that wet reduction does not change the position of the low temperature reduction peak and moves the high temperature reduction peak to slightly higher temperature (about 30 °C). The oxidation peak observed at 760 °C in Figure 12 during dry re-oxidation of wet reduced catalyst is similar to the oxidation peak observed in Figure 7 for the wet re-oxidation of dry reduced catalyst, but occurs at a slightly higher temperature. The quantitative results presented in Figures 9 and 14 indicate that the amount of wet reduction obtained both at low temperature (around 150 °C) and high temperature (around 450 °C) is somewhat higher than those for the dry reduction. On the other hand, the wet TPR of dry re-oxidized catalyst shown in Figure 13 is significantly different compared to the dry TPR of the wet re-oxidized catalyst given in Figure 8. The low temperature peak observed at 150 °C during the wet or dry TPR of the fresh catalyst re-appears in the wet reduction of the dry re-oxidized catalyst, and the high temperature reduction peak that was seen starting around 750 °C in Figures 3 and 8, starts at around 500 °C in Figure 13 and peaks at around 850 °C. When the quantitative results presented in Figures 10 and 15 are compared, it is seen that the total amounts of reduction of the re-oxidized catalyst in both cases are comparable.The results shown in Figures 16-20 for the wet reduction, wet re-oxidation case are almost identical to the results of wet reduction, dry re-oxidation case presented in Figures 11-15.

In summary, the presence of water vapor during the reduction and/or re-oxidation of the catalyst plays a significant role in retaining the reduction-oxidation activity of the catalyst. While about the same amount of reduction is obtained for dry reduction-wet re-oxidation and wet reduction-dry or wet re-oxidation cases, the reduction temperatures are significantly lower for the wet reduction cases.

From these observations it may be tentatively concluded that the effect of water vapor during reduction is to reduce sintering and retain reduction and oxidation activity at lower temperatures while the effect of water vapor during re-oxidation may be attributed to the enhancement of the oxidation rate by the presence of OH groups.

TPR of Other Catalysts Prepared by NASA/LaRC

Figure 21 shows the dry TPR of the baseline 15% Pt/SnO_2 catalyst with hydrogen and Figures 22-26 show the TPR curves for various combinations of tin oxide with the oxides of cerium, zirconium and aluminum.

Table 1. Summary of TPR Results for Various Tin Oxide-Based Mixed Oxide Catalysts

Catalyst	First Peak Temp. Range (pk temp), °C	Second Peak Temp. Range (pk temp), °C	First Peak Size ml STP H_2/100 mg cat.	2nd Peak Size ml STP H_2/ 100 mg cat.	Total reduction ml STP H_2/ 100 mg cat.
15% Pt/SnO_2	44-222 (148)	280-544 (456)	2.68	7.93	10.6
Sn (011019/1)	150–350 (250)	440–690 (613)	1.36	12.4	13.8
Sn/Ce (011019/2)	175-437 (248, 330)	500-760 (642)	2.05	13.5	15.6
Sn/Ce/Zr (011019/3)	135-330 (238)	390-706 (540)	2.24	11.1	13.3
Sn/Ce/Zr/Al (011019/4)	152-440 (304)	447-840 (600)	2.43	4.65	7.08
Sn/Zr (011019/5)	150-430 (290)	490-670 (600)	5.78	12.3	18.1

Since the amount of tin oxide in each mixture is different, relative amounts of reduction cannot be observed directly from these figures. Therefore, the quantitative results are calculated and presented in Table 1 along with the information about the reduction peak temperatures. The lowest reduction peak temperatures are obtained with the Pt-containing baseline catalyst. The other catalysts have significantly higher peak temperatures, low around 300 °C and high around 600 °C, with the exception of Sn/ Ce/Zr catalyst, which has reduction peaks around 240 °C and 540 °C. An interesting observation from the table is the increase in the amounts of both low and high temperature reductions for Sn/Zr catalyst and the increase in the amount of high temperature reduction for the Sn/Ce This can be attributed to the ability to create oxygen vacancies and high oxygen mobility of the cerium and zirconium oxides.

These observations make the investigation of the enhancement of the activity and high temperature stability of tin oxide-based catalysts by the introduction of appropriate metal oxides an attractive topic for future investigations.

TPD of Other Catalysts Prepared by NASA/LaRC

For these experiments the catalyst sample was subjected to various pretreatments. Pretreatments with dry gases consisted of flowing a gas stream (He, He+10.1% CO, He+3.6% O_2) over the catalyst sample for two hours at 50 °C. Pretreatment with wet He involved flowing dry He over the catalyst for 2 hours followed by a 10-minute flow of He bubbled through de- ionized water at 25 °C. All pretreatments were followed by He flow over the catalyst at 50 °C for two hours to desorb the physically adsorbed species. This was followed by the injection of 1-ml doses of the CO-containing

gas into the carrier gas stream at 30 °C. This dosing was continued until the peak areas stayed relatively constant. Only CO_2 was observed in the exit gas, using a gas chromatograph equipped with a thermal conductivity detector, indicating that the catalyst was very effective in oxidizing CO. The CO_2 peaks eventually reached a relatively constant area, which was smaller than the CO peak of the feed.

Figure 27 shows the temperature programmed desorption results for catalyst samples subjected to various pretreatments. The TPD results were different after the pretreatment of the catalyst in He, CO, O_2, and wet He. Two desorption peaks were obtained with the catalysts pretreated with dry gases, while only the first desorption peak was obtained with the catalyst pretreated with wet He. The low temperature peak observed around 75 °C for dry He and CO pre-treatment and at 100 °C for O_2 pre-treatment was tentatively attributed to the desorption of physically adsorbed species. The absence of this low temperature peak for the TPD of the catalyst sample pretreated with wet He can be explained by the filling of active sites with adsorbed water. Due to the presence of the cold trap the desorption of water is not observed. The high temperature peak observed around 225-250 °C was attributed to the formation and subsequent desorption of CO_2. Two possible mechanisms may be possible for the formation of CO_2. One may be through the reaction of a CO molecule adsorbed on a platinum site with the lattice oxygen of an adjacent tin oxide site. Another route to CO_2 formation may be the formation of surface carbonates at the metal oxide sites and the subsequent decomposition of these surface carbonates. The slightly elevated temperature of the second peak for oxygen pretreatment will be consistent with this second mechanism. These arguments are based on the gas chromatographic analysis of desorption products, which indicated the presence of only CO_2; but the analysis of the desorption products were not detailed enough to arrive at a more definite conclusion. Figure 28 shows the effect of pretreatment temperature on the TPD results after CO pre-treatment. The low temperature desorption peak is absent for pretreatment at 125 °C because the pretreatment temperature is higher than the temperature for the desorption of physically adsorbed species. The difference in the shapes of the desorption curves for the 50 °C and 125 °C pre-treatment with CO may be due to the decrease of the importance of CO_2 formation through the first mechanism as the result of the decrease in the amount of CO adsorbing at Pt sites at the high pre-treatment temperature. After the TPD runs up to 600 °C the catalysts were re-oxidized with oxygen at 600 °C and the re-oxidized catalysts produced TPD curves with no peaks indicating very slow, almost constant rate desorption (Figure 29).

Temperature Programmed Reaction Studies with GC-MS Analyzer

Since the results of the gas chromatographic analyses were not sufficiently sensitive to provide an accurate gas compositions, it was decided to replace the gas chromatograph with a new GC-mass spectrometer system for more detailed product gas analysis and to repeat the CO chemisorption-TPD runs under He-O_2 mixture to obtain more insight into the processes occurring on the catalyst.

Figure 30 shows the relative amounts of CO and CO_2 obtained when the fresh 15 % Pt/SnO_2 catalyst was subjected to repeated 0.993 ml doses of 10.1 % CO in He under flowing He at 50 °C. The corresponding thermal conductivity detector peak areas indicating the total gas composition change are also shown. It is seen that negligible amounts of CO are present in the product gases and almost all the injected CO is oxidized to CO_2 possibly through the formation and subsequent decomposition of tin carbonates. Figure 31 shows the TPD curve obtained after the CO injections of Figure 30, while the relative amounts of the evolved species are presented in Figure 32. These figures show that the first TPD peak below 100 °C is due to the desorption of adsorbed air and moisture and the peak around 220 °C is due to the CO_2 evolution as the result of the dissociation of surface carbonate

species. No significant quantities of CO were detected. Following the TPD of Figure 31, TPO of the catalyst was performed up to 530 °C. Figure 33 shows the relative amounts of CO and CO_2 obtained when the re-oxidized catalyst was subjected to repeated 0.993 ml doses of 10.1 % CO in He under flowing He at 50 °C. Deactivation of the catalyst is clearly visible. A significant amount of CO is observed along with the CO_2 (the ratio of CO to CO_2 is about 2:3). The following TPD produced a flat curve and the analysis of the gases did not show any presence of CO or CO_2 indicating the absence of carbonate species on the surface. This observation combined with Figure 33 implies that not all CO_2 was formed by the dissociation of the carbonates, but the reduced catalyst has some activity for direct CO oxidation as well, possibly involving Pt surface sites.

Figure 34 shows the TPD curve obtained after CO chemisorption under a carrier gas containing 3.6 % O_2 in He. This is very similar to Figure 32 except that the observed peak temperature is slightly higher. The species evolved during TPD is presented in Figure 35. The most important observation from this figure is the small CO peak occurring at the same temperature as the CO_2 peak. Figures 36 and 37 show the species produced with fresh and used catalyst during the injection of 0.993 ml doses of CO under an oxygen-containing gas stream at 50 °C, respectively. With the fresh catalyst no CO is observed and the CO_2 evolution decreases slightly to a steady state value after about 6 injections. On the other hand, with the used catalyst the CO_2 evolution increases from zero to about the same steady state value after about 14 injections, while the observed CO, which is initially about one third of the steady state CO_2 value, decreases continuously with each CO dose. Apparently, presence of oxygen in the feed inhibits the deactivation of the catalyst, which maintains significant activity even when heated up to 530 °C. This may be attributed either to the involvement of gaseous oxygen in the oxidation of CO on the Pt sites, or to the enhancement of the CO oxidation by the oxygen in the gas phase, which fills the oxygen vacancies created in the tin oxide lattice when a CO molecule on the Pt surface reacts with the lattice oxygen of an adjacent metal oxide site.

Figure 38 shows the species evolved during 0.993-ml injections of 10.1 % CO in He at 50 °C into a carrier gas stream of moist He containing 2.8 % water vapor. As with the other carrier gas streams almost all CO is oxidized to CO_2. The amount of CO observed is slightly more than those when dry and oxygen-containing helium is used as the carrier gas stream. Figure 39 shows the TPD curve obtained after CO chemisorption under a carrier gas containing 2.8% H_2O in He. The desorption peak occurs at the same temperature as with dry He, but the size of the peak is significantly smaller. The species evolved during desorption is very similar to those observed after CO injections under oxygen-containing carrier gas, but the amounts are much smaller (Figure 40). From these observations it can be concluded that presence of water during CO injections inhibit surface carbonate formation, thus the much smaller desorption peak, but enhance direct CO oxidation on the Pt sites with water supplying the oxygen by some sort of water gas shift mechanism, as evidenced by the high conversion to CO_2 shown in Figure 38.

CONCLUSIONS

The main conclusion from the TPR experiments is that the presence of water during reduction, re-oxidation, or both helps the 15 % Pt/SnO_2 catalyst to retain its oxidation-reduction activity even when heated up to about 1000 °C. This is attributed to the presence of hydroxyl groups attached to tin oxide, which may facilitate the re-oxidation of the reduced oxide.

The TPD and TPRn results indicate the existence of two different mechanisms for the oxidation of CO on the

15 % Pt/SnO_2 catalyst. One mainly involves the platinum sites and leads to the oxidation of adsorbed CO either by the lattice oxygen supplied by a neighboring tin oxide site or an adsorbed oxygen atom, the second going through the formation of surface carbonates and their subsequent desorption. The extremely high conversion rate for the fresh catalyst during CO injections and the relatively lower conversion rate on the re-oxidized catalyst indicate the importance of the first mechanism. The second mechanism is the primary source of CO_2 that is observed during temperature programmed desorption.

Both the presence of oxygen or water facilitates the first mechanism by providing external oxygen. High temperature reduction appears to kill the catalyst's activity for the carbonate formation but the catalyst maintains its ability to promote CO oxidation via the first mechanism.

Presence of water vapor during CO oxidation diminishes carbonate formation significantly. This is rather disappointing because water vapor was also found to facilitate the re-oxidation of the catalyst and help retain its reduction-oxidation activity. This indicates the need for finding an appropriate additive to retain the catalyst activity in high temperature applications. Oxides like ceria, which possess a large oxygen capacity, high oxygen mobility, and the ability to form oxygen vacancies, are prime candidates for this purpose. Preliminary TPR studies presented in this report for the effect of some additives indicate that results with ceria and zirconia are very promising. Finding an optimum catalyst composition will be the focus of future activities.

FIGURES

Figure1. Dry TPR of Fresh 15 % Pt/SnO_2 Catalyst. Temperature plot (TPRPS04)

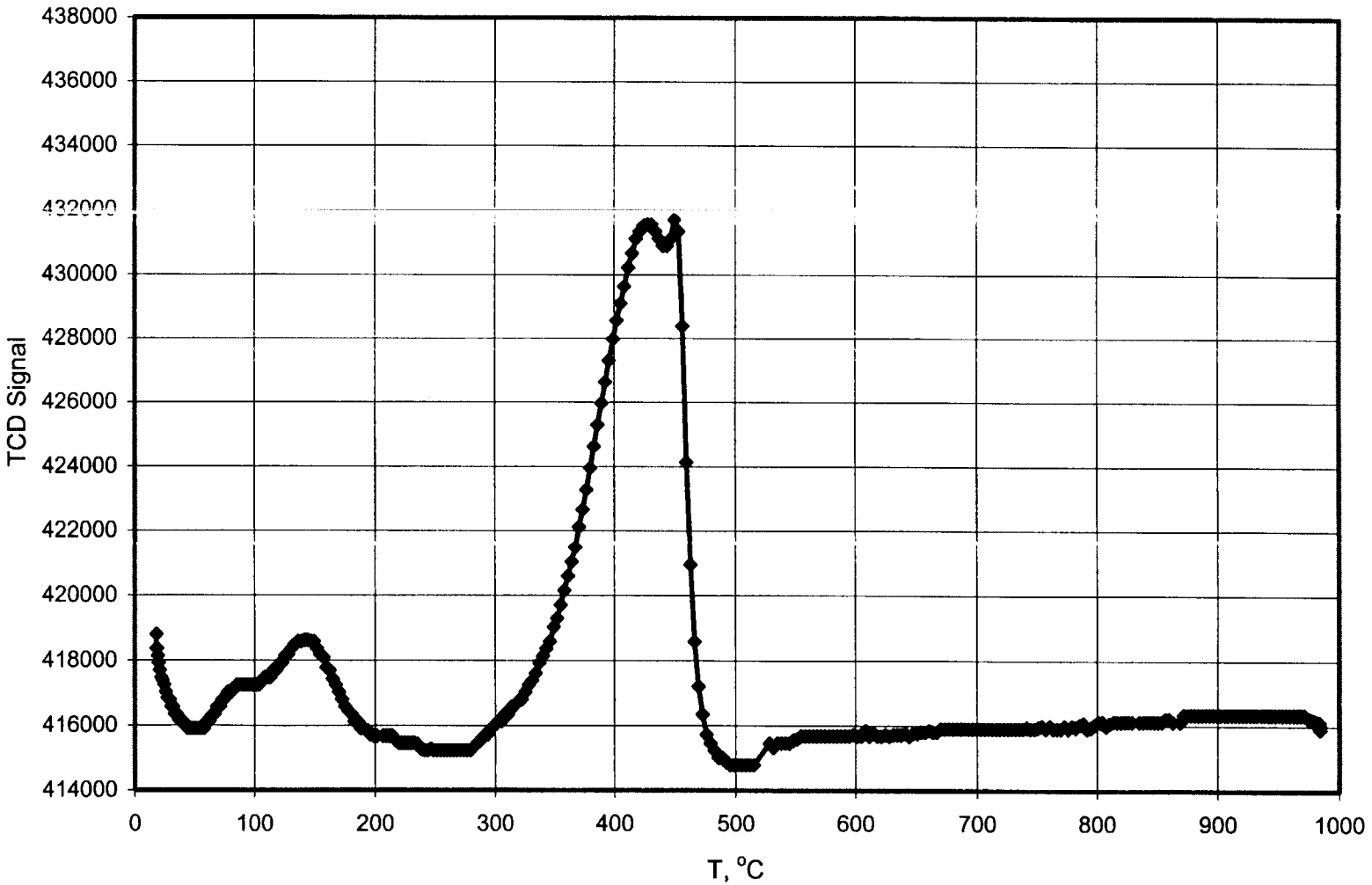

Figure 2. Dry Reoxidation of Dry-Reduced 15 % Pt/SnO_2 Catalyst Temperature plot (TPRPS04A)

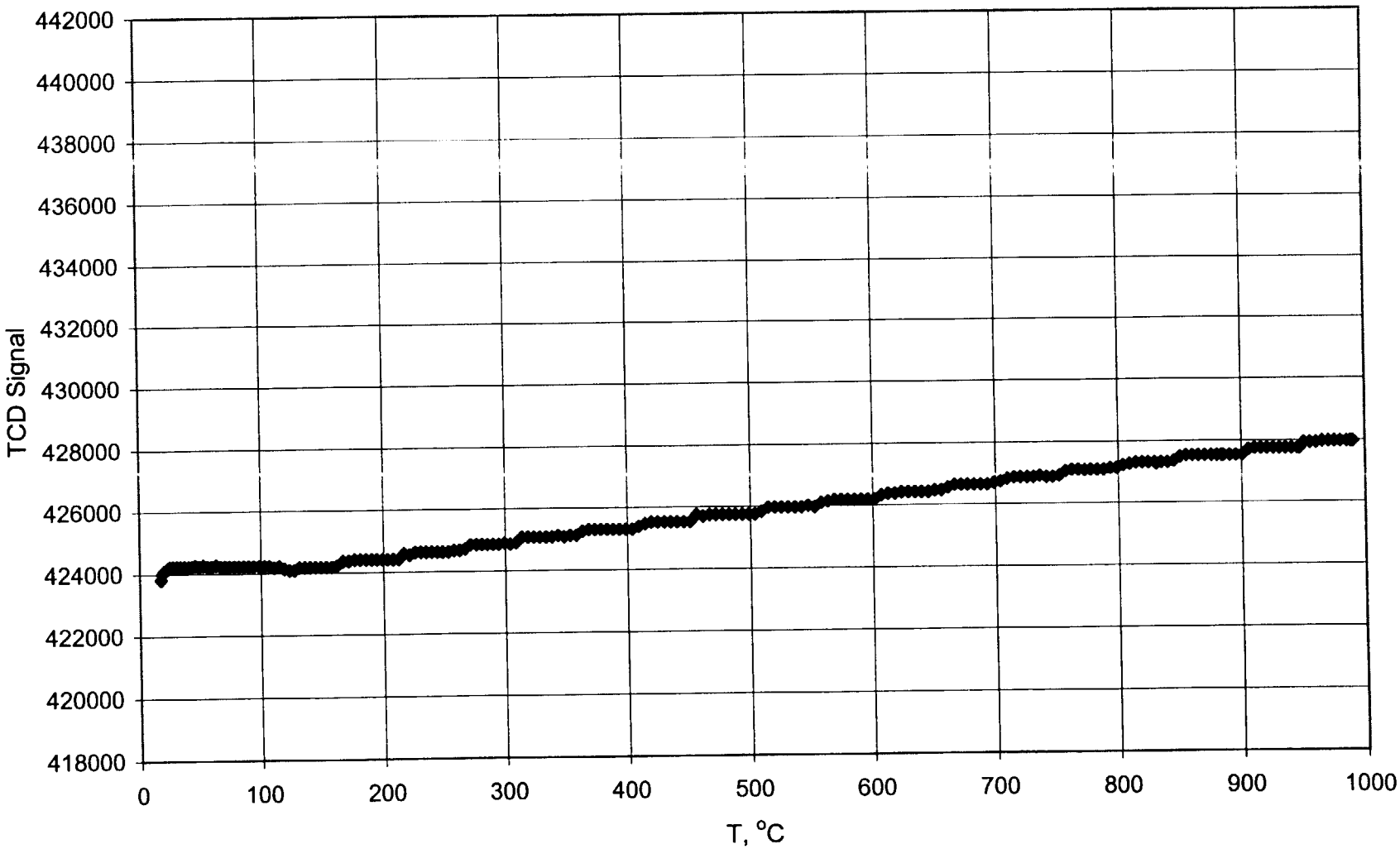

Figure 3. Dry TPR of Dry Reoxidized 15 % Pt/SnO_2 Catalyst. Temperature plot (TPRPS04B)

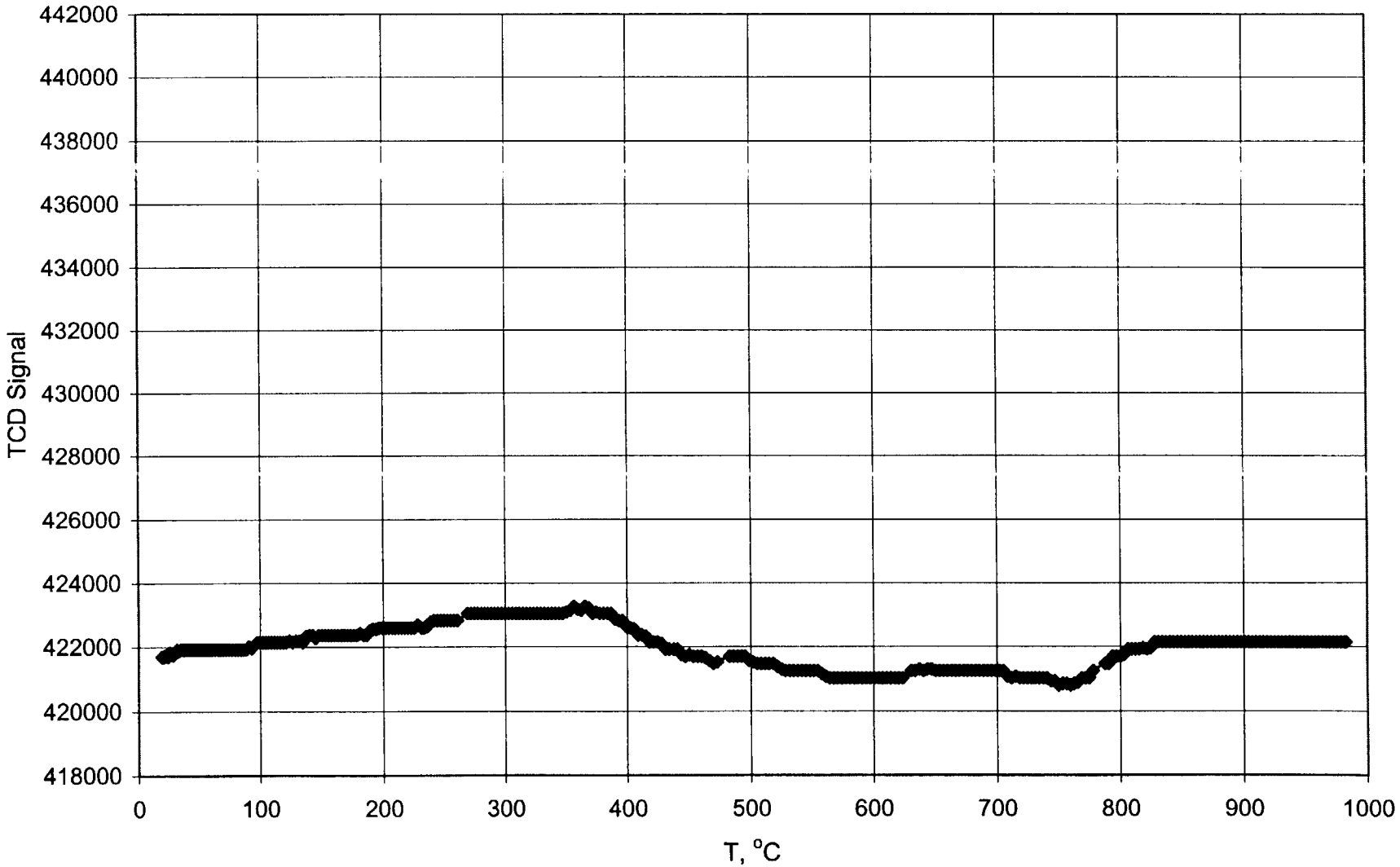

Figure 4. Dry TPR of Fresh 15 % Pt/SnO2 Catalyst. Time plot (TPRPS04)

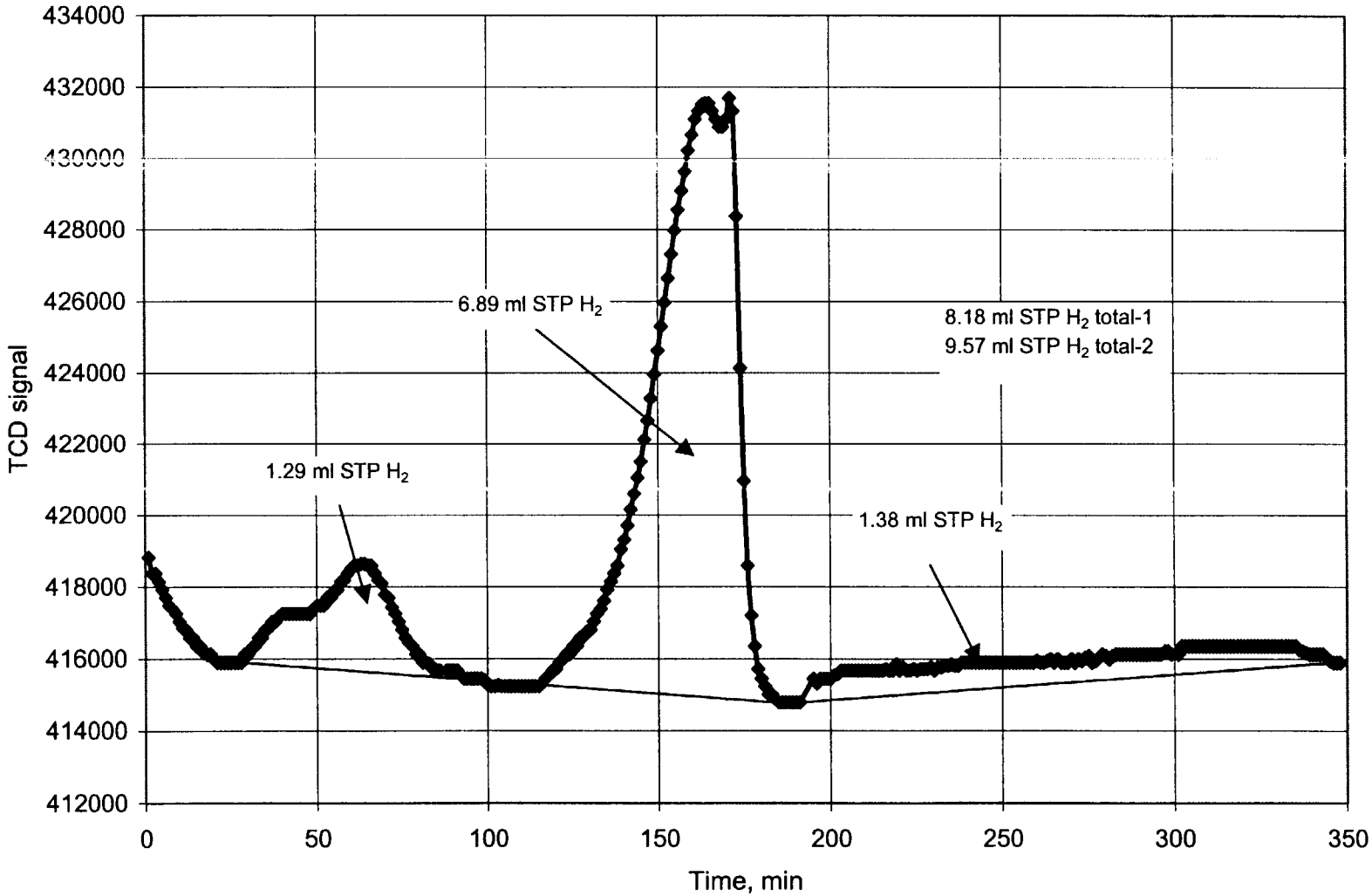

Figure 5. Dry TPR of Dry Reoxidized 15 % Pt/SnO2 Catalyst. Time plot (TPRPS04B)

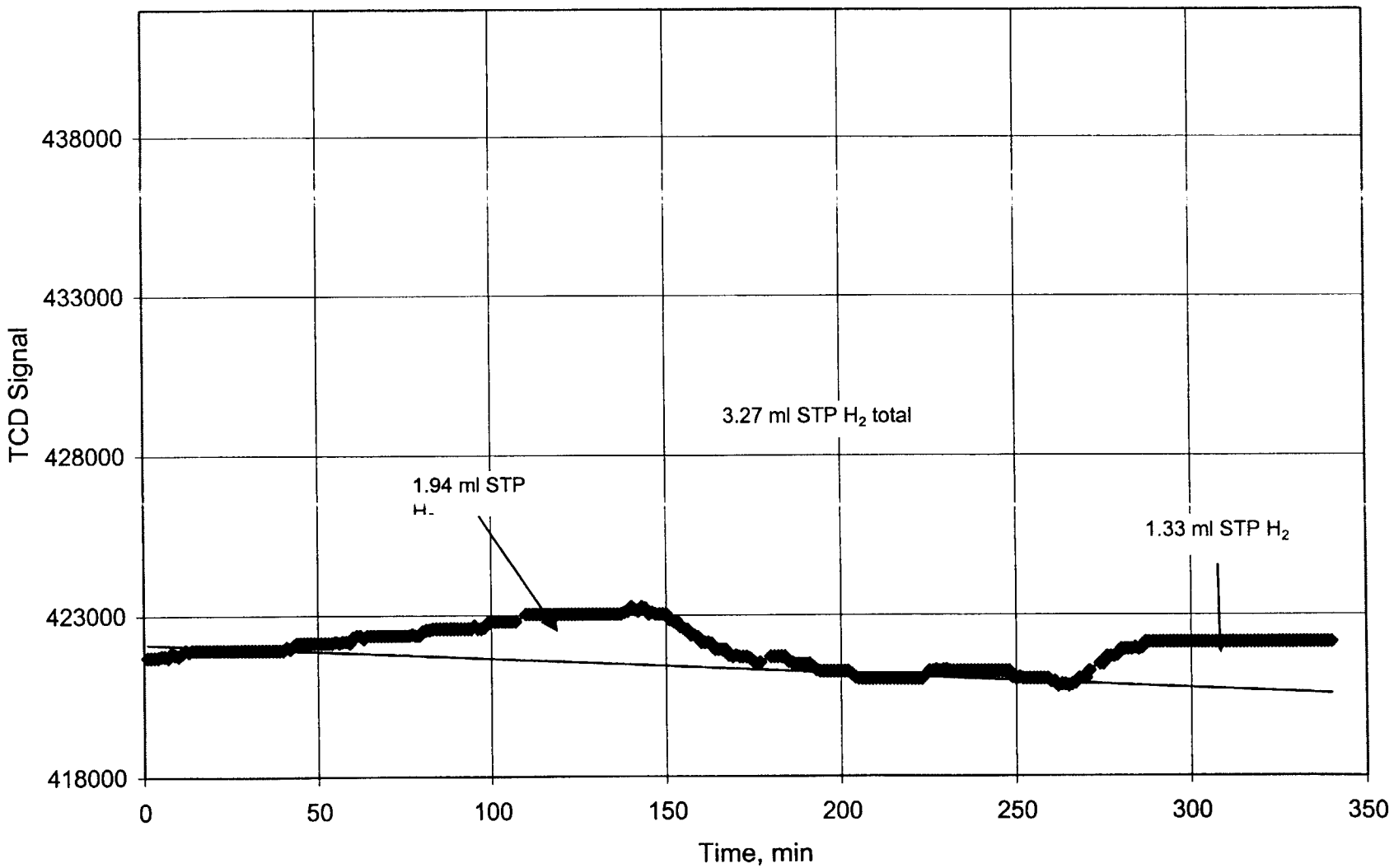

Figure 6. Dry TPR of Fresh 15 % Pt/SnO_2 Catalyst. Temperature plot (TPRPS01)

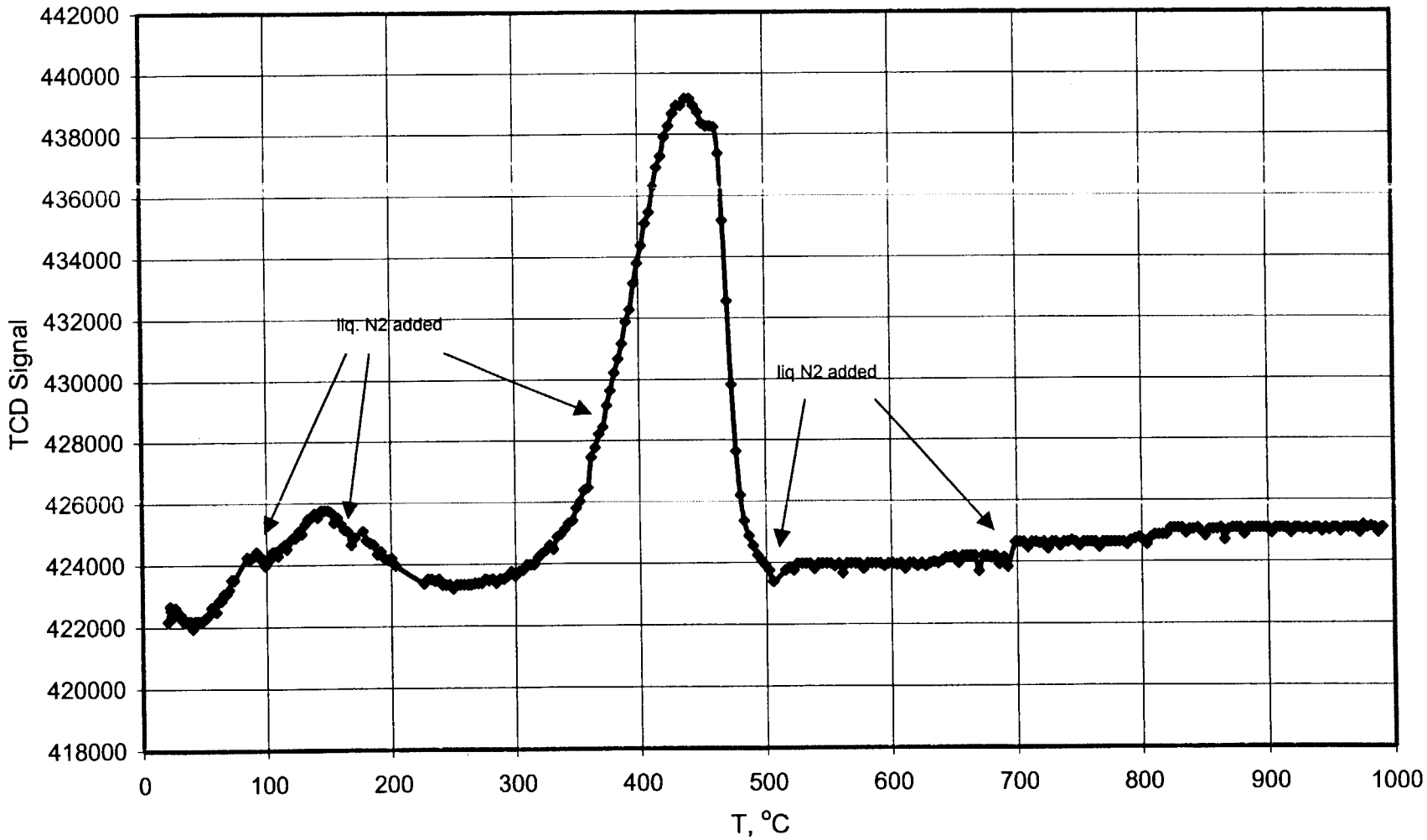

Figure 7. Wet TPO of Dry-Reduced 15% Pt/SnO_2 Catalyst. Temperature plot (TPRPS01A)

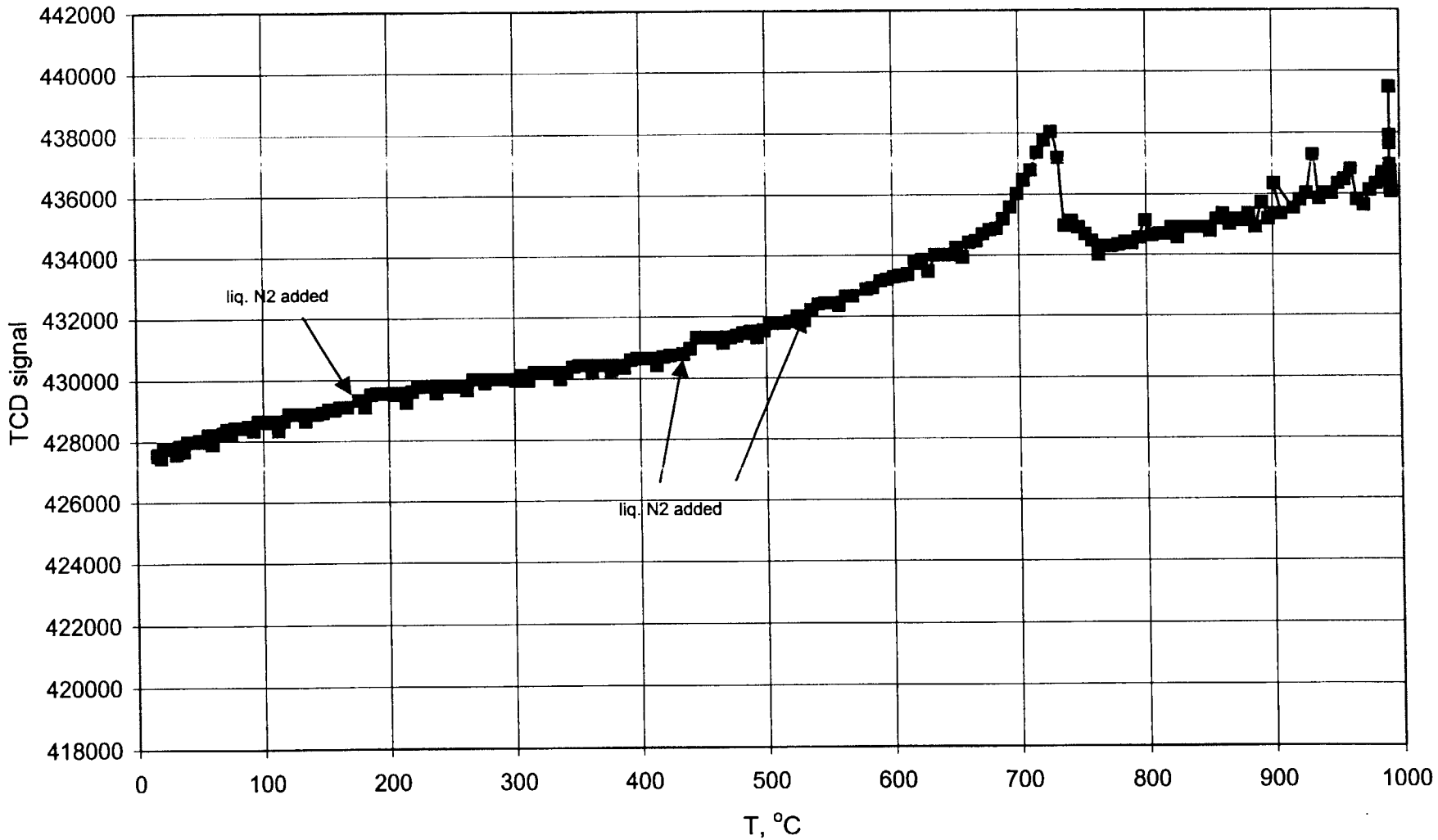

Figure 8. Dry TPR of Wet-Reoxidized 15 % Pt/SnO_2 Catalyst. Temperature plot (TPRPS01B)

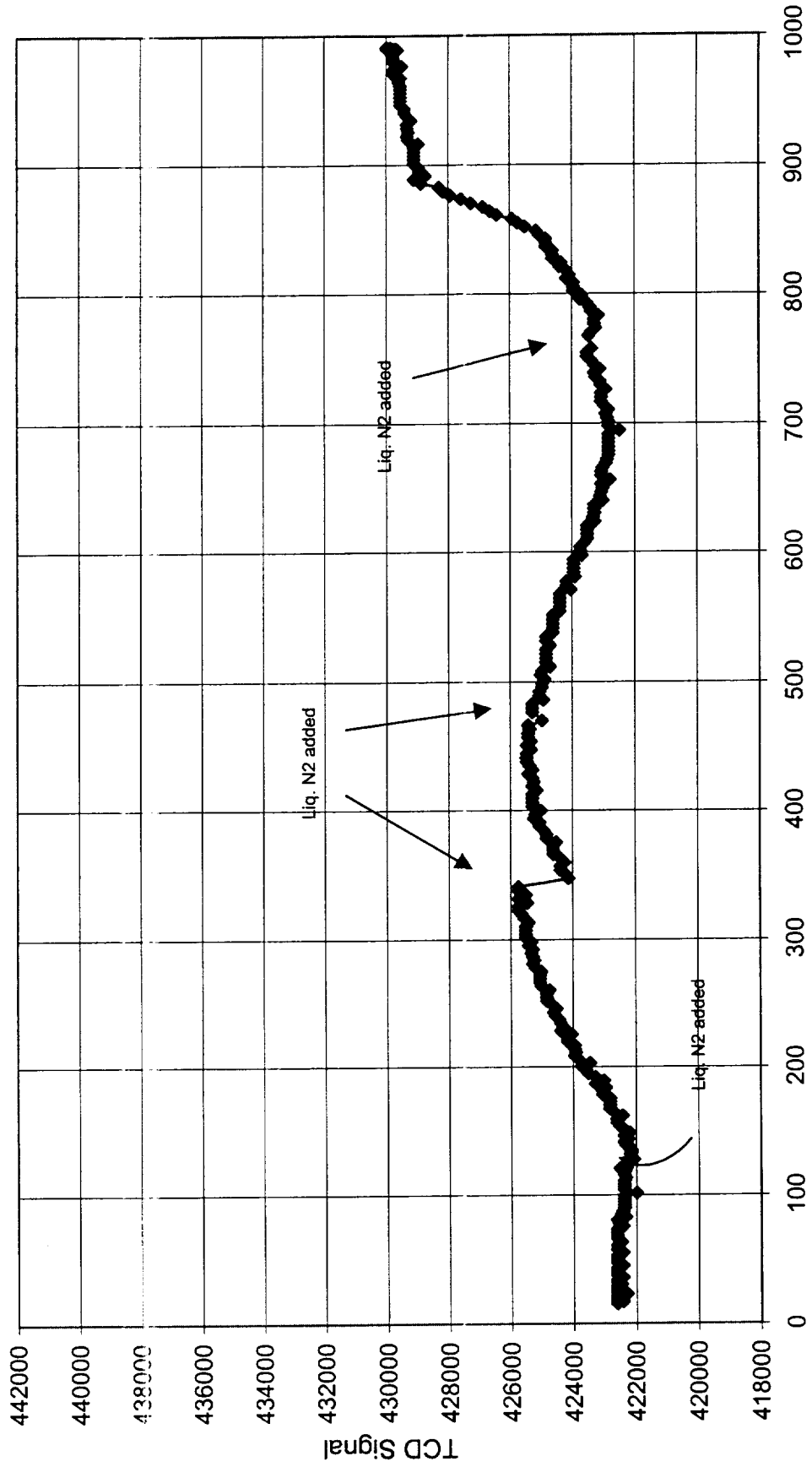

Figure 9. Dry TPR of Fresh 15 % Pt/SnO2 Catalyst. Time plot (TPRPS01)

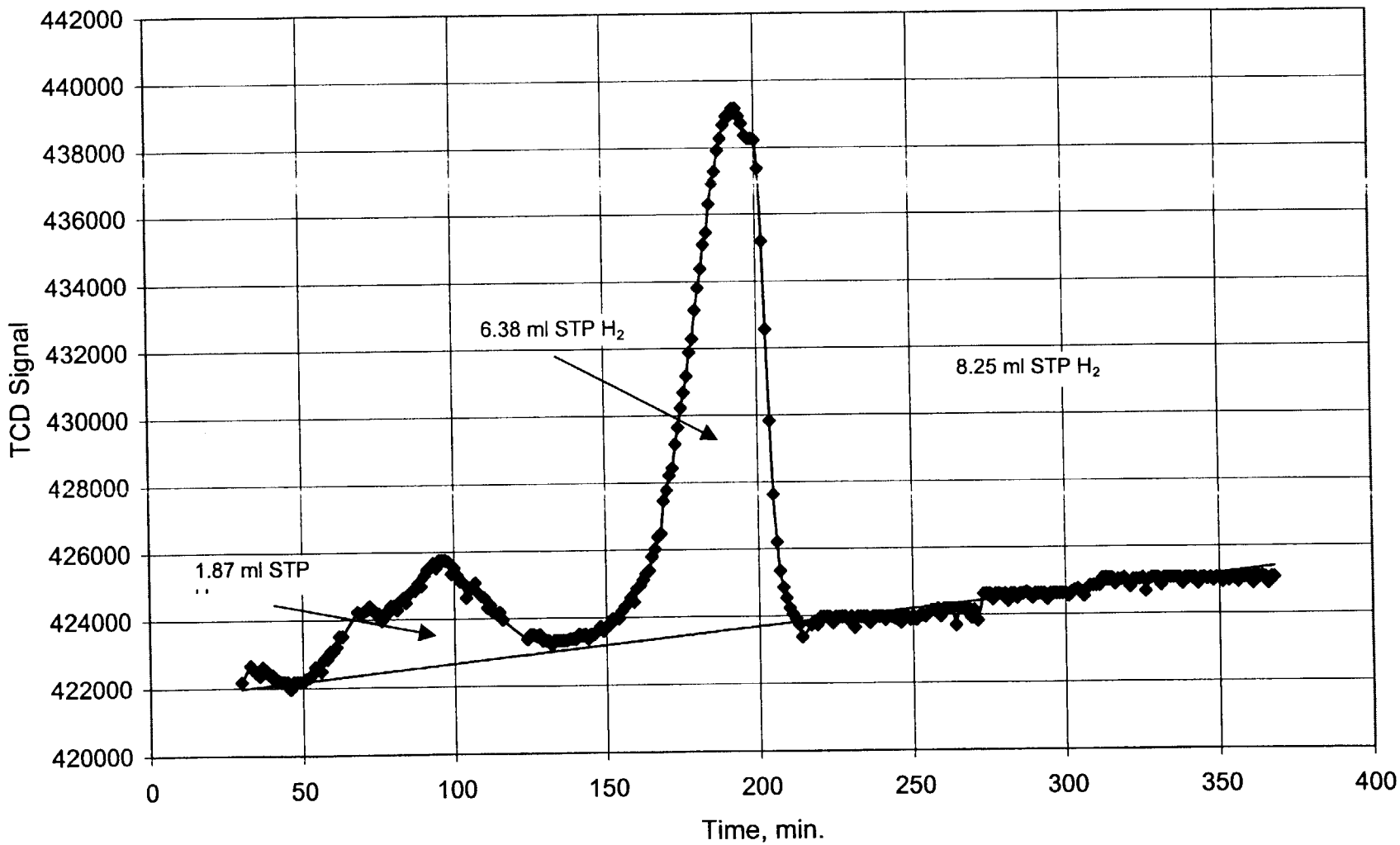

Figure10. Dry TPR of Wet Reoxidized 15% Pt/SnO2 Catalyst. Time plot (Adj-1) (TPRPS01B)

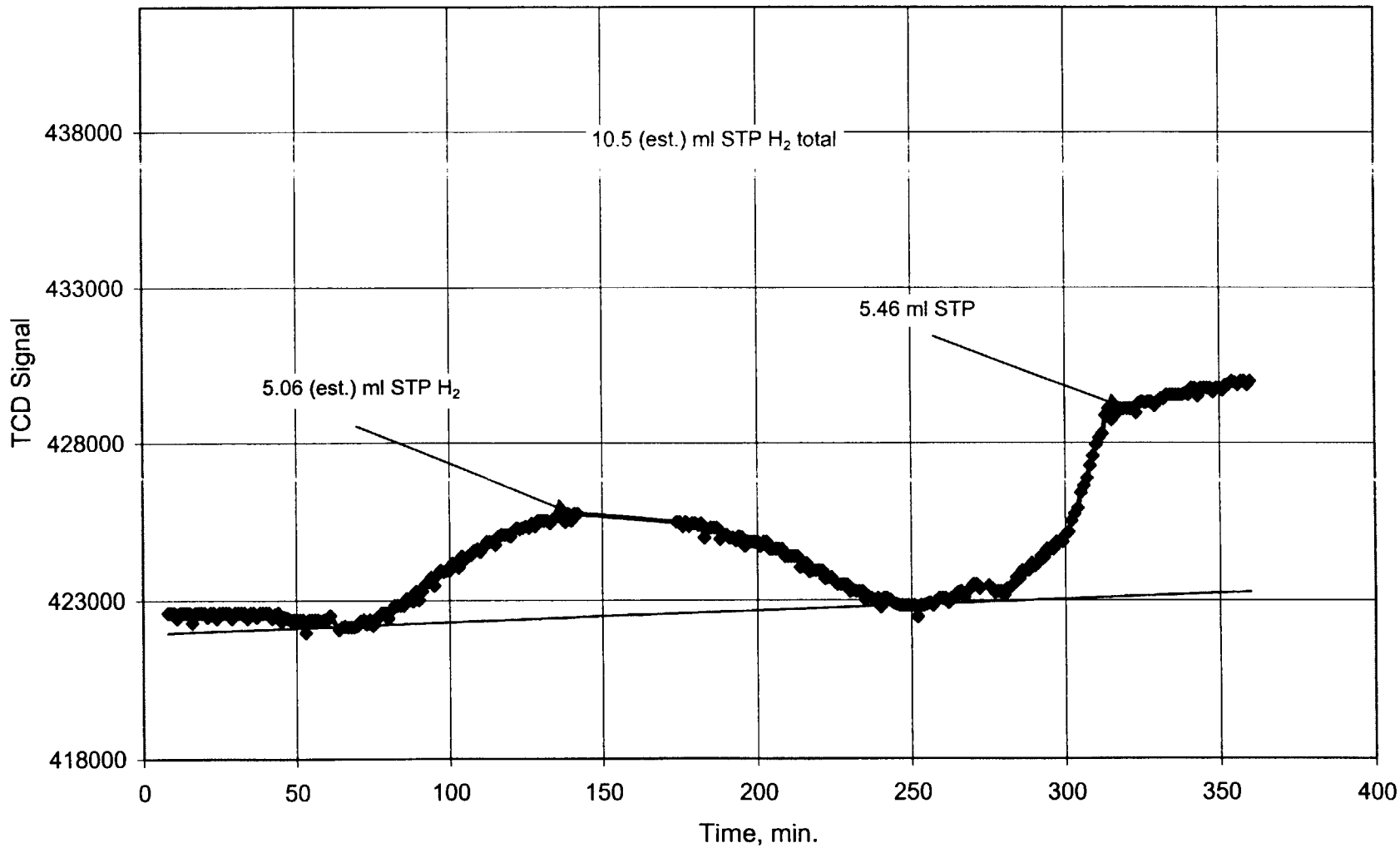

Figure 11. Wet TPR of Fresh 15 % Pt/SnO_2 Catalyst. Temperature plot (TPRPS03)

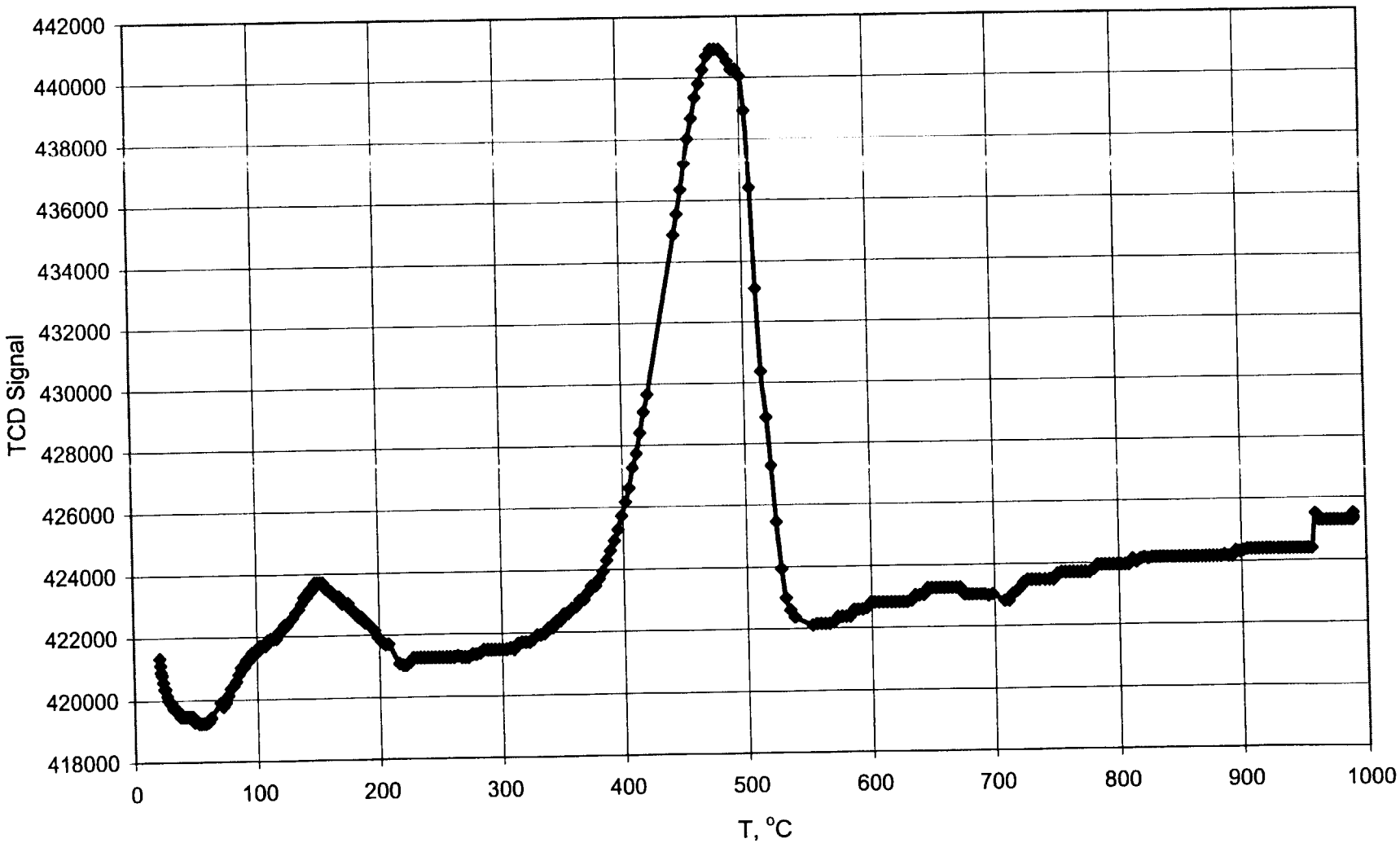

Figure 12. Dry TPO of Wet-Reduced 15% Pt/SnO_2 Catalyst.Temperature plot (TPRPS03A)

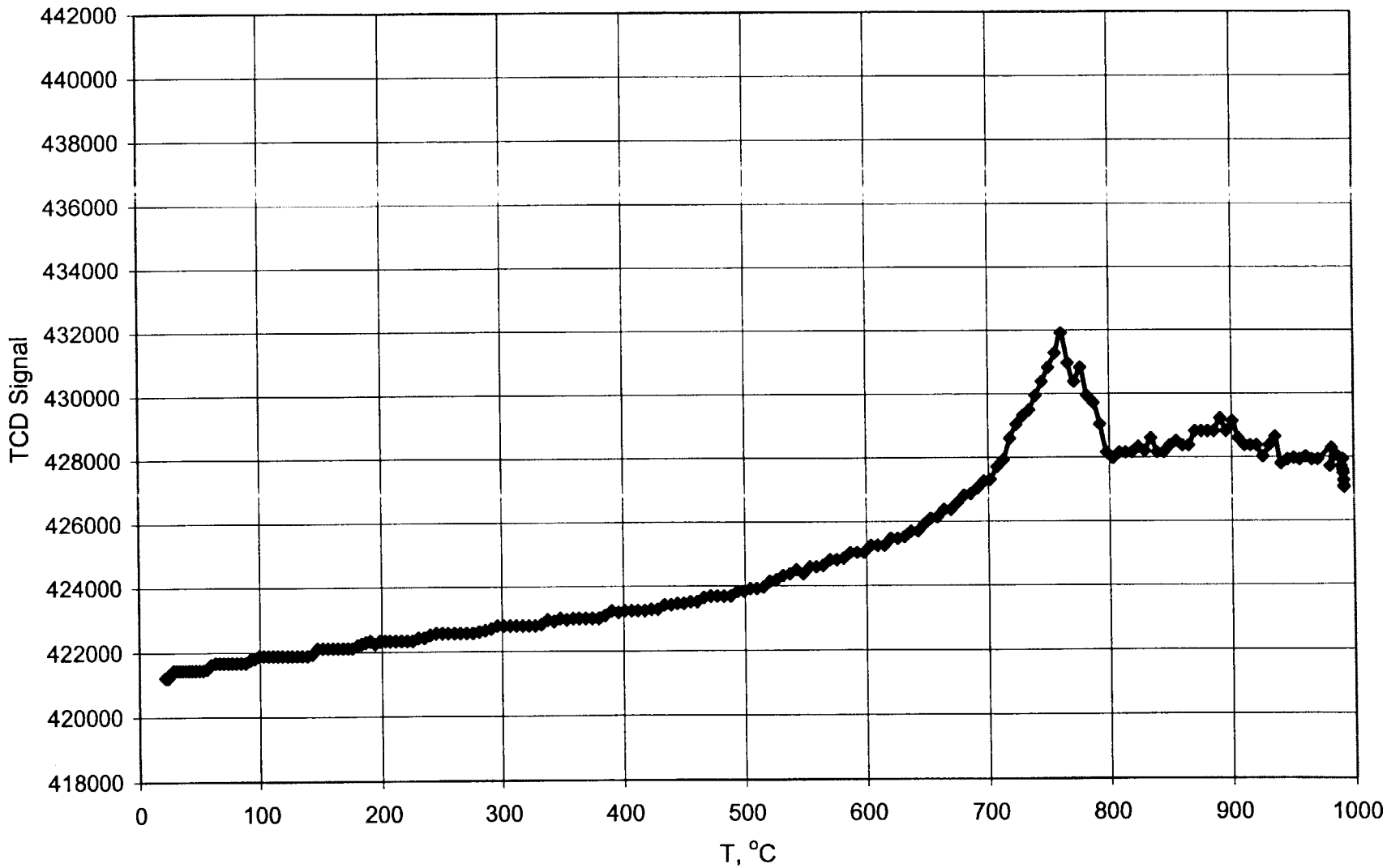

Figure 13. Wet TPR of Wet-Reduced, Dry-Reoxidized 15 % Pt/SnO_2 Catalyst.Temperature plot (TPRPS03B)

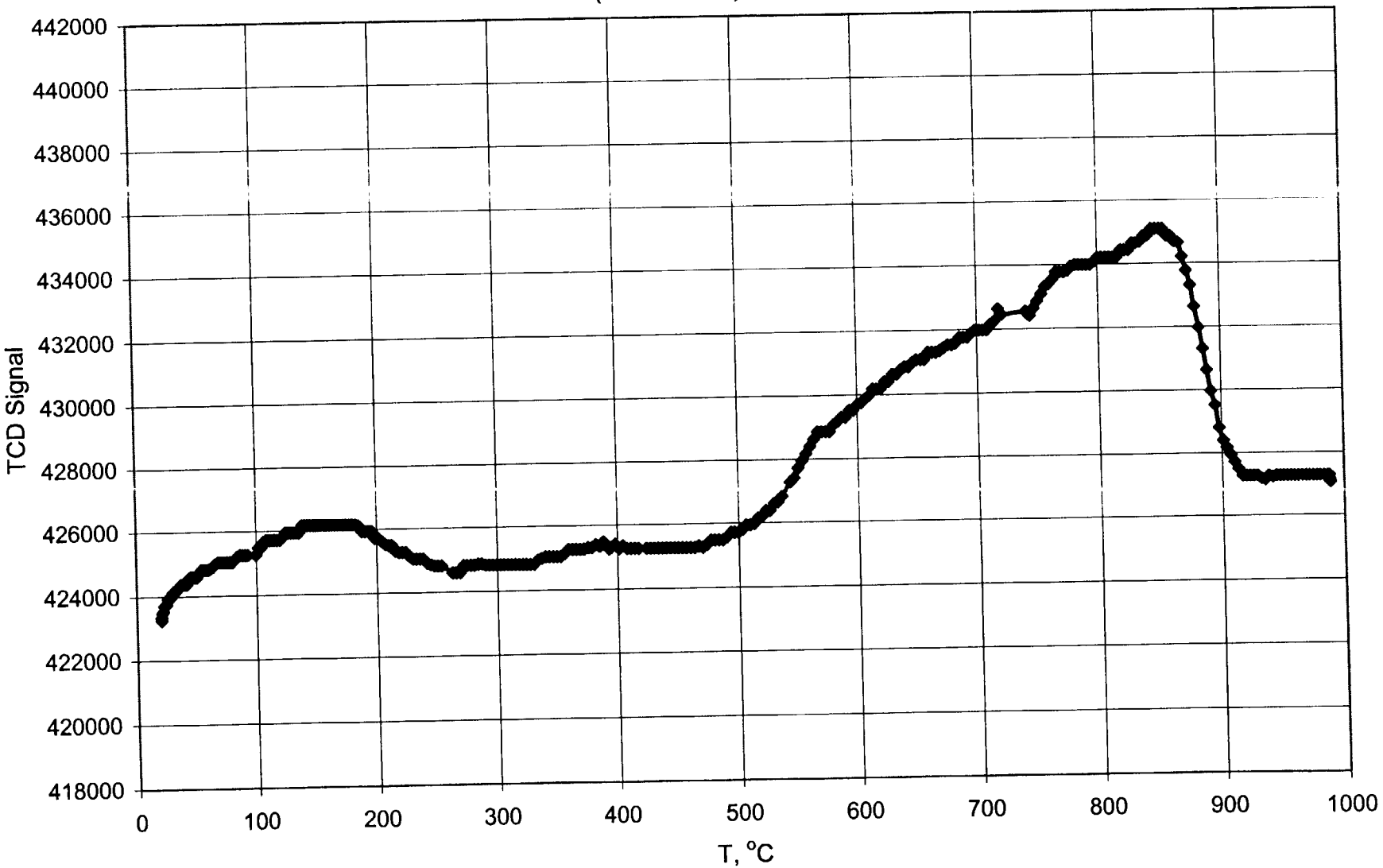

Figure 14. Wet TPR of Fresh 15 % Pt/SnO2 Catalyst. Time plot (TPRPS03)

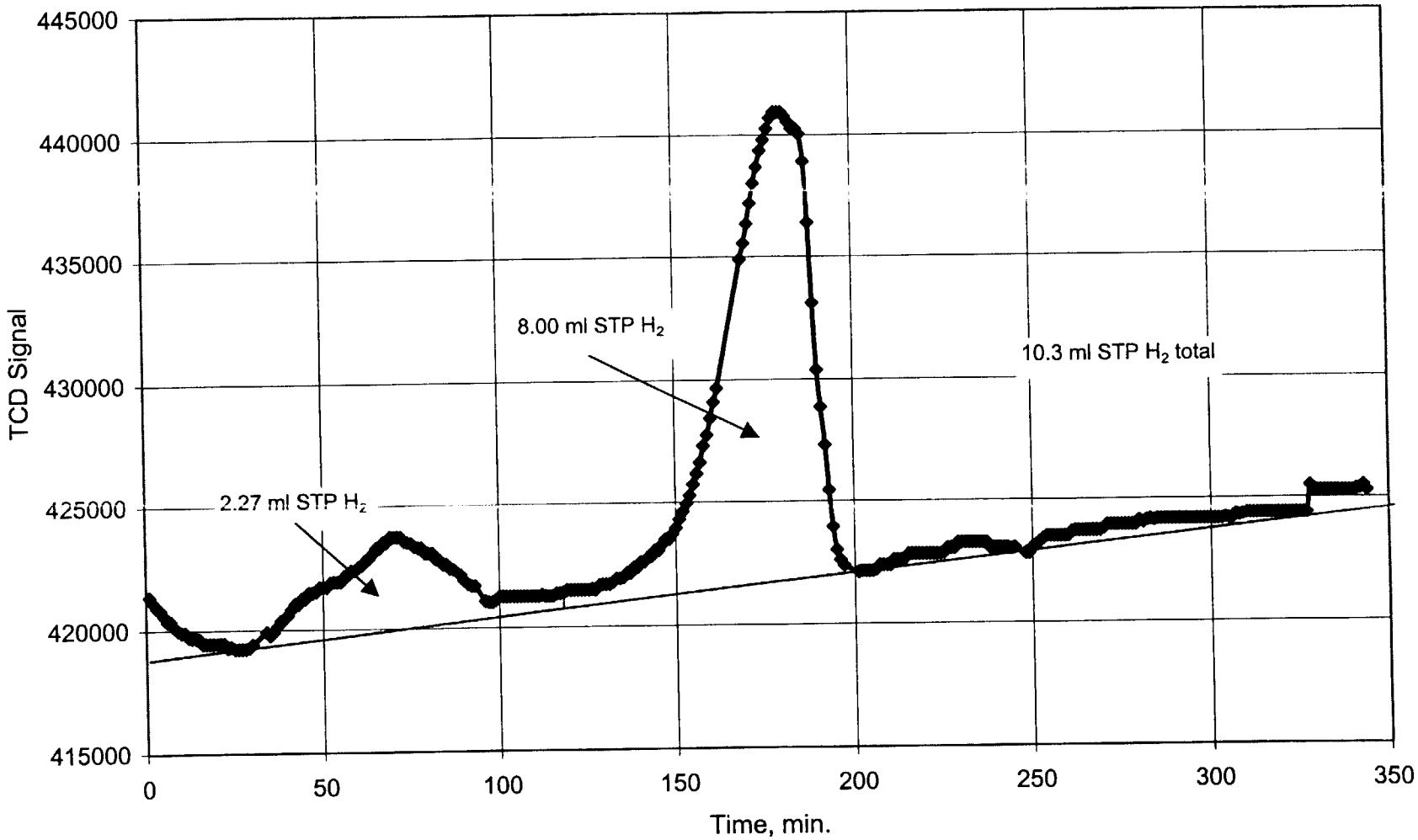

Figure 15. Wet TPR of Wet-Reduced, Dry-Reoxidized 15 % Pt/SnO2 Catalyst. Time plot (TPRPS03B)

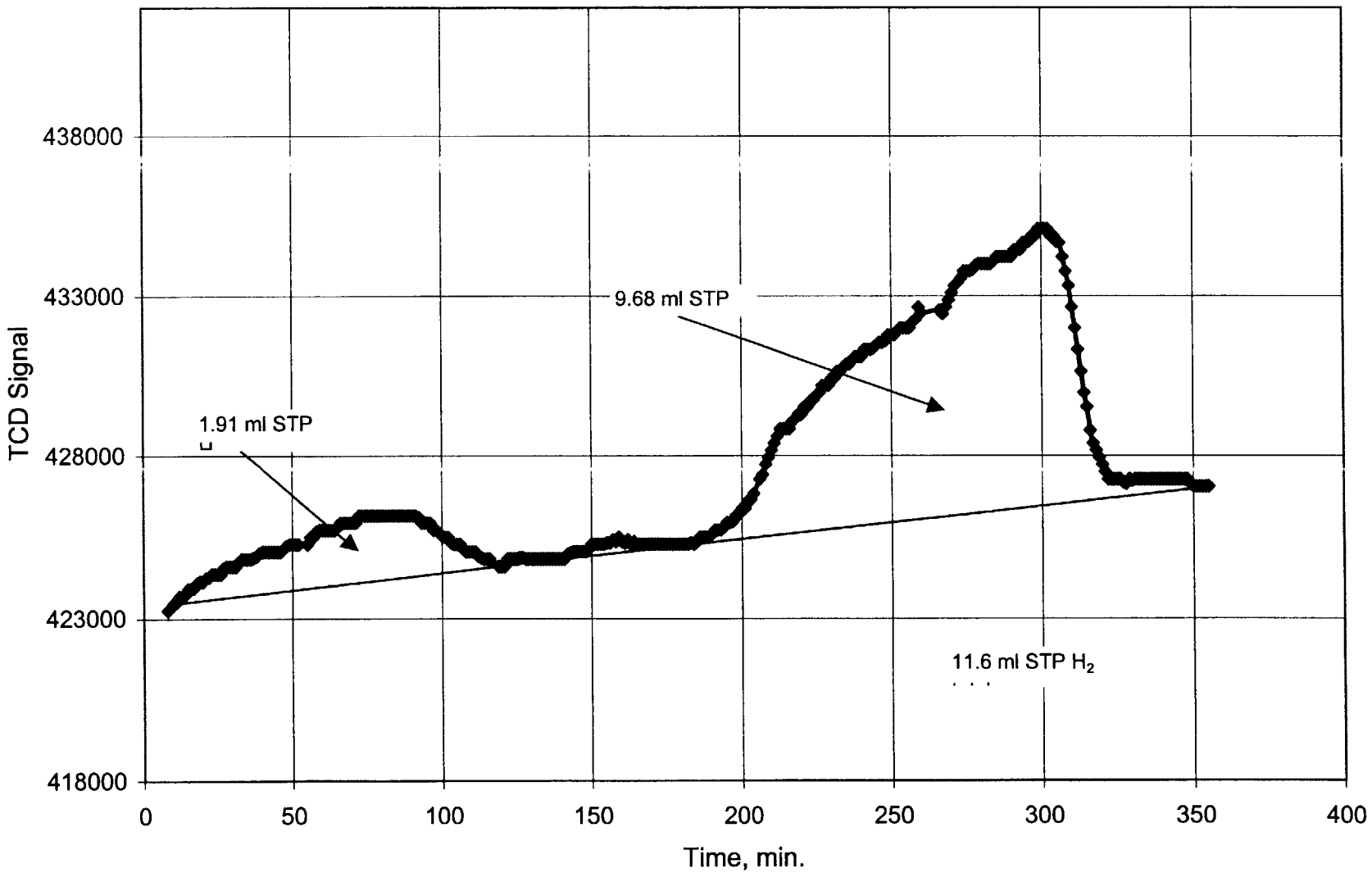

Figure 16. Wet TPR of Fresh 15 % Pt/SnO_2 CatalystTemperature plot (TPRPS02)

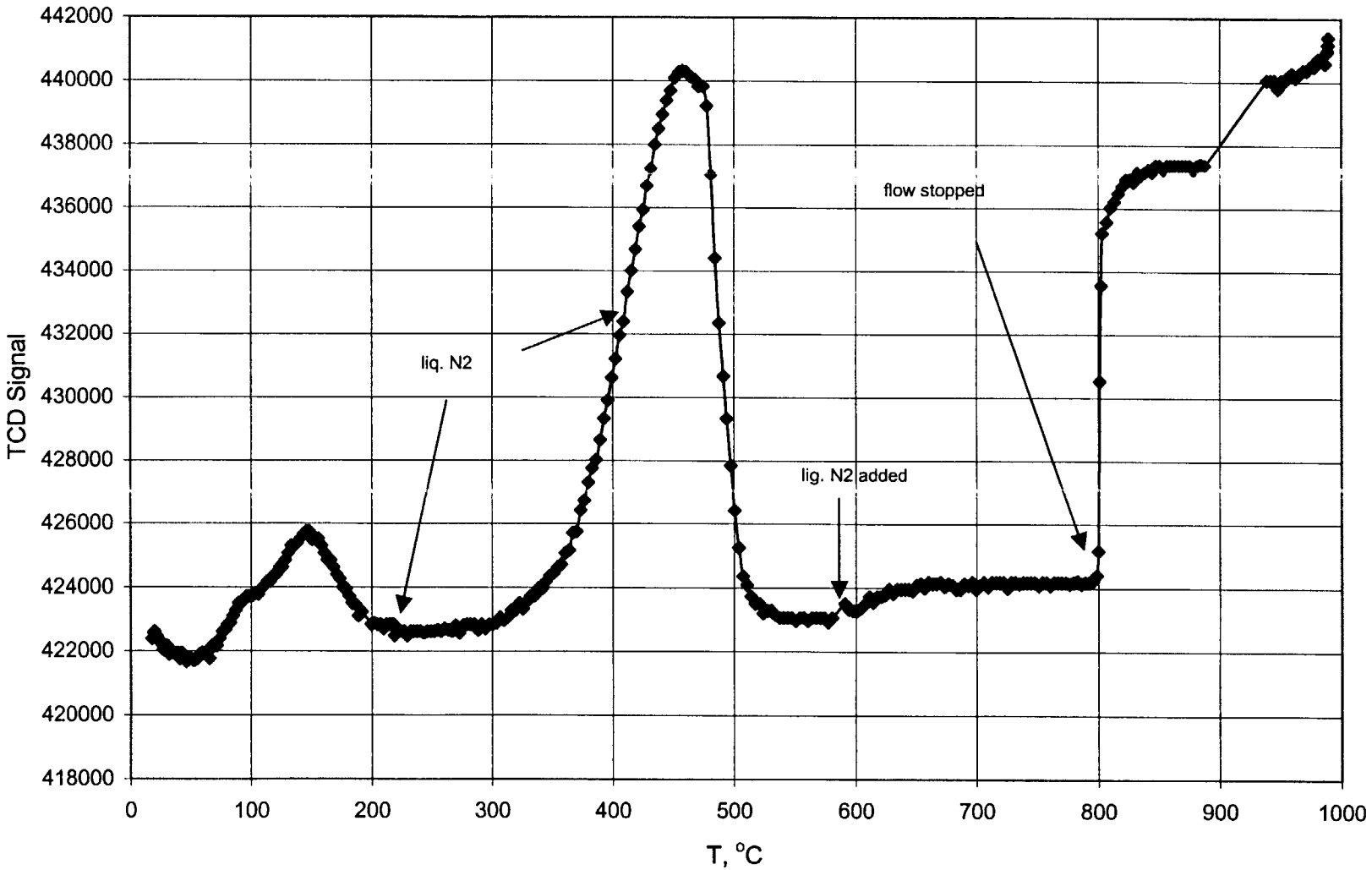

Figure 17. Wet-Reoxidation of 15 % Pt/SnO_2 Catalyst After Wet TPR. Temperature plot (TPRPS02A)

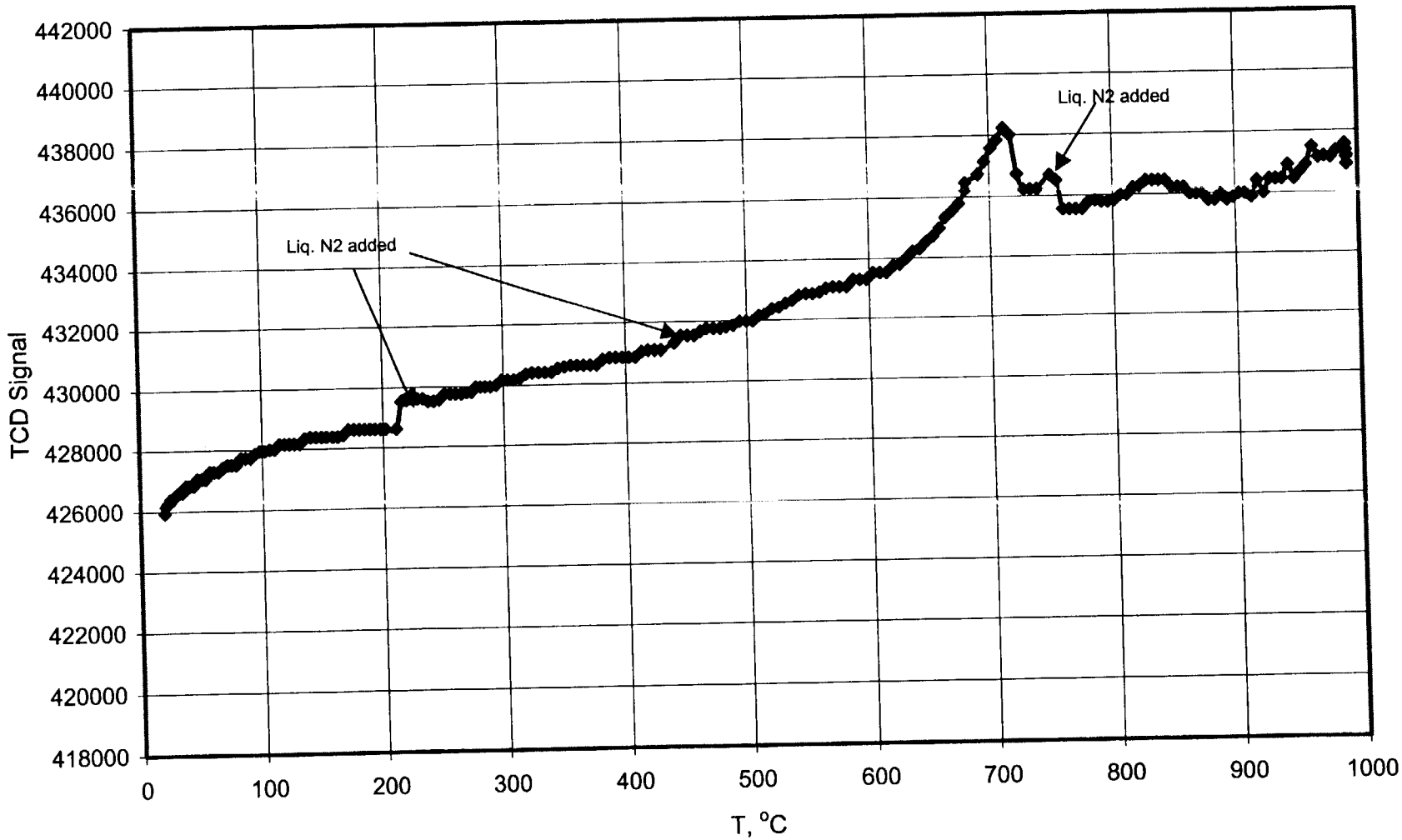

Figure 18. Wet TPR of Wet-Reduced, Wet-Reoxidized 15 % Pt/SnO_2 Catalyst. Temperature plot (TPRPS02B)

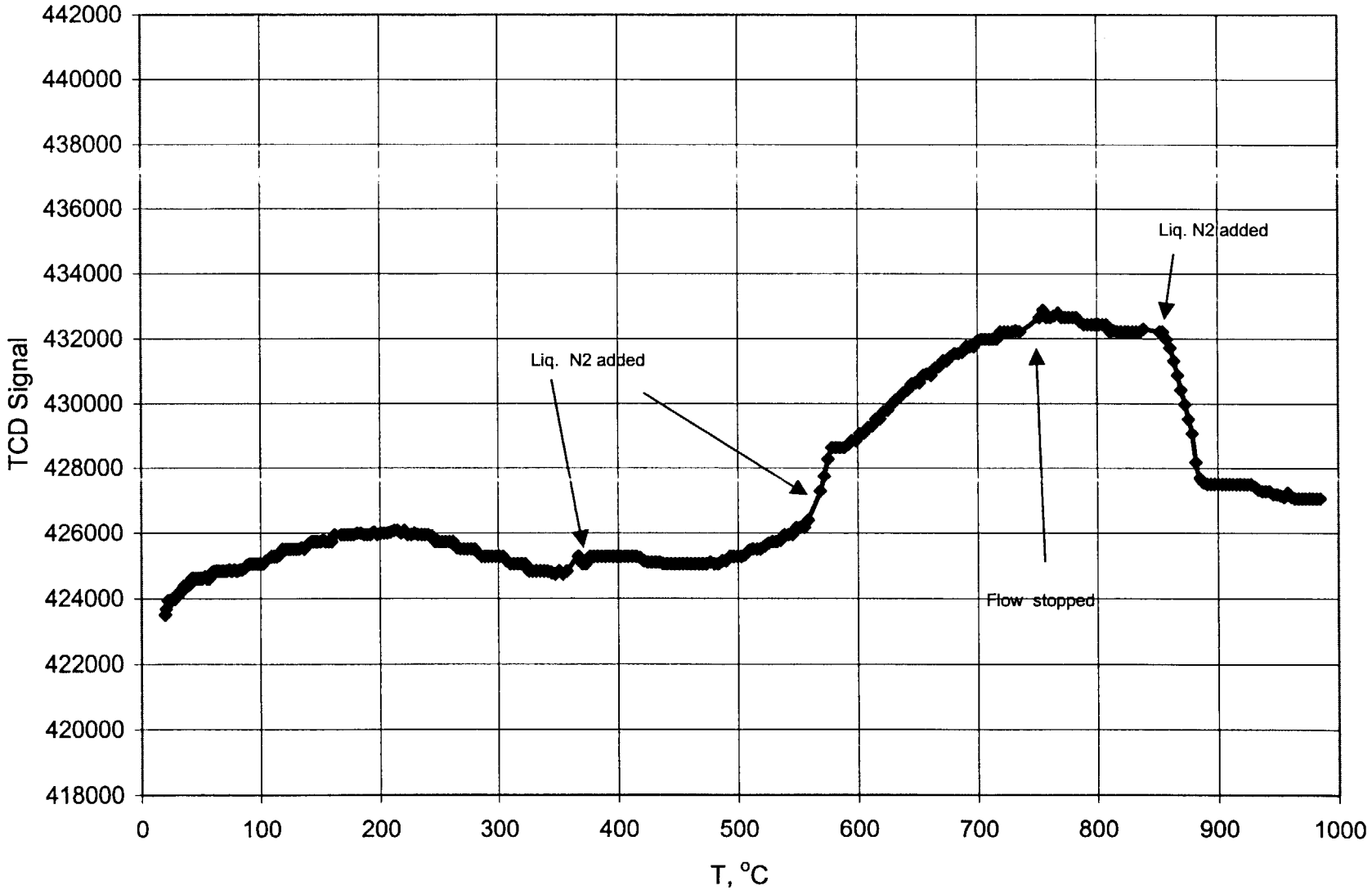

Figure 19. Wet TPR of Fresh 15 % Pt/SnO2 Catalyst. Time plot (TPRPS02)

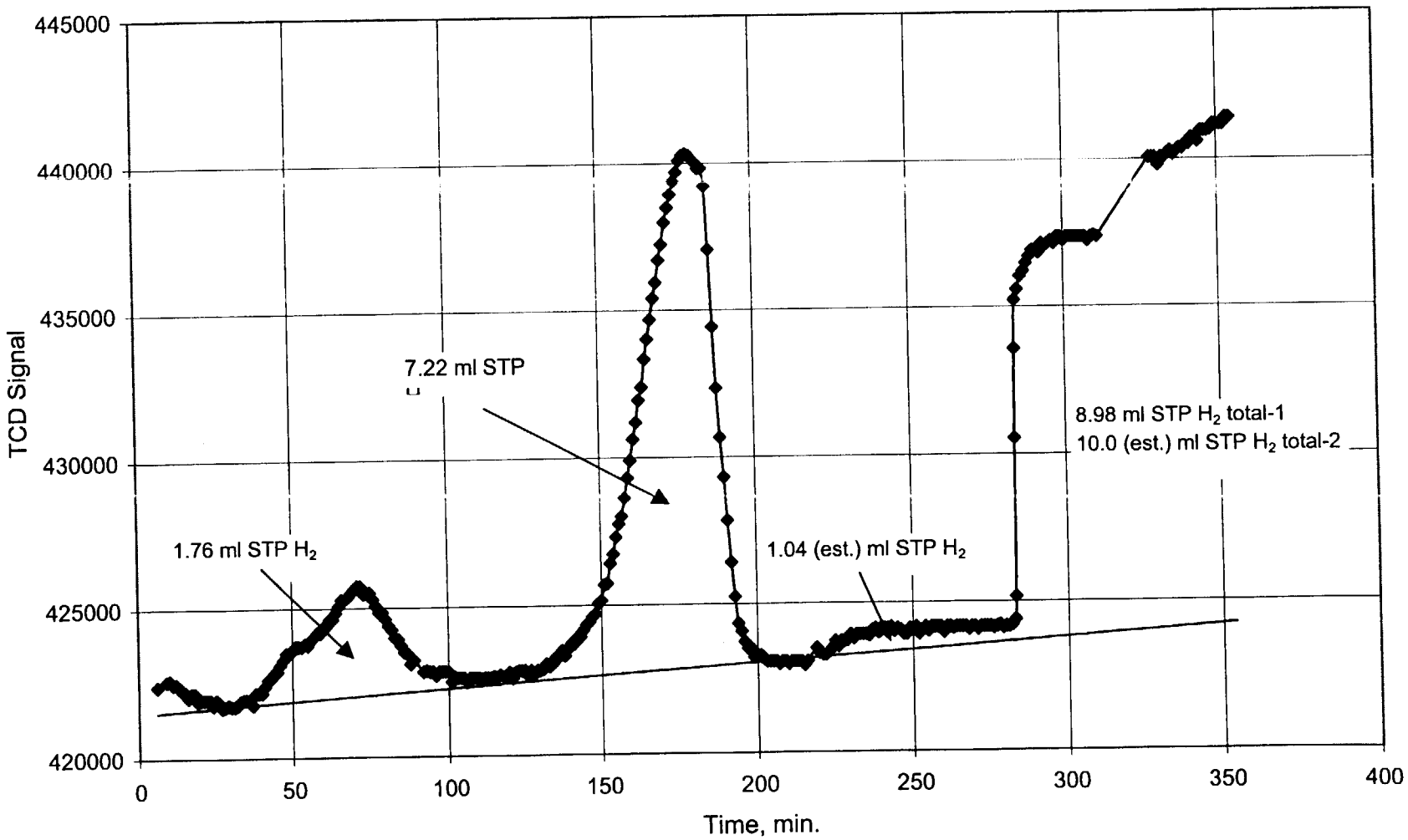

Figure 20. Wet TPR of Wet-Reduced, Wet-Reoxidized 15 % Pt/SnO2 Catalyst. Time plot (TPRPS02B)

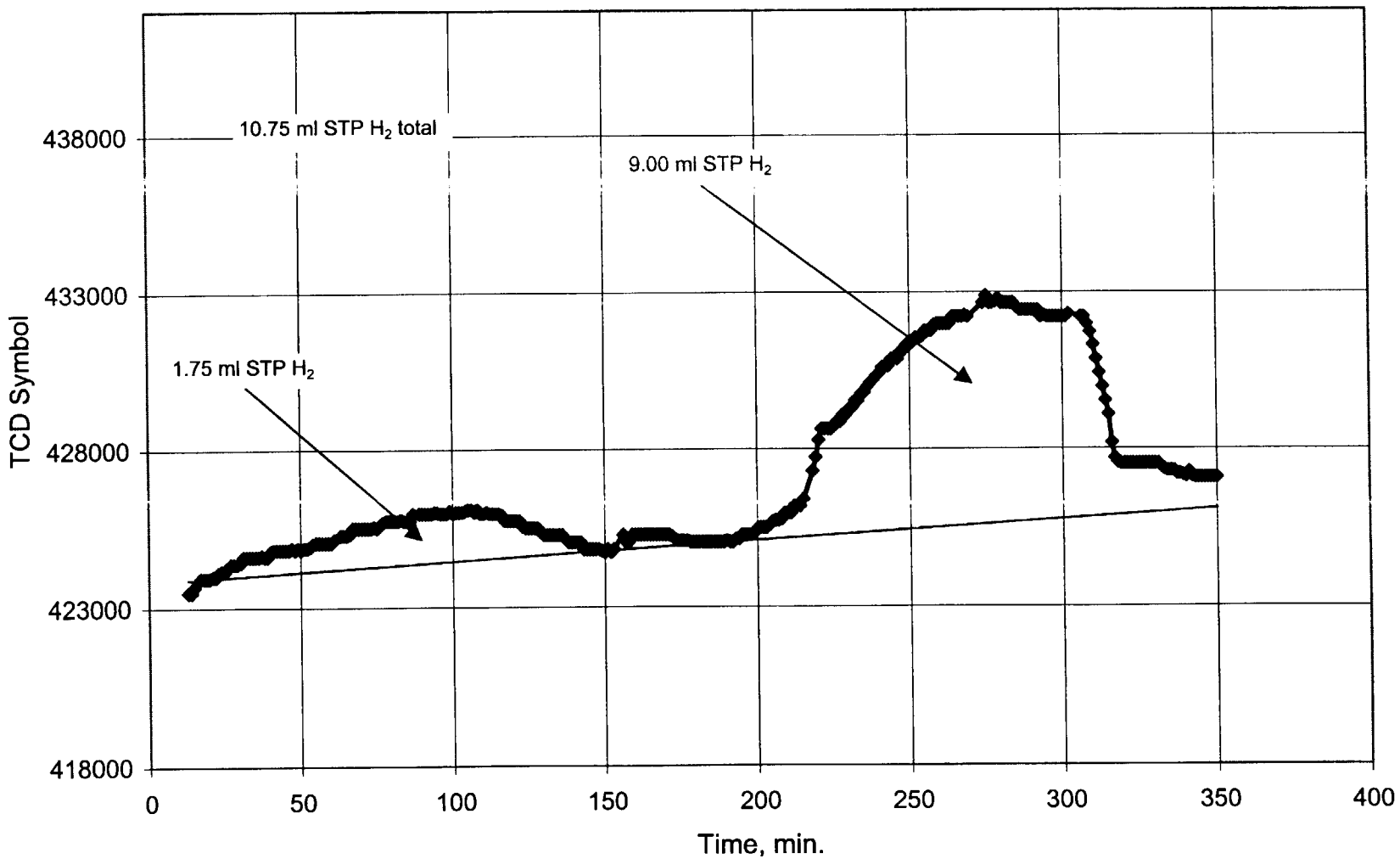

Figure 21. TPR of 15 % Pt/SnO_2 Catalyst with 6.69 % H2 in Ar. Catalyst mass = 0.0483 g.

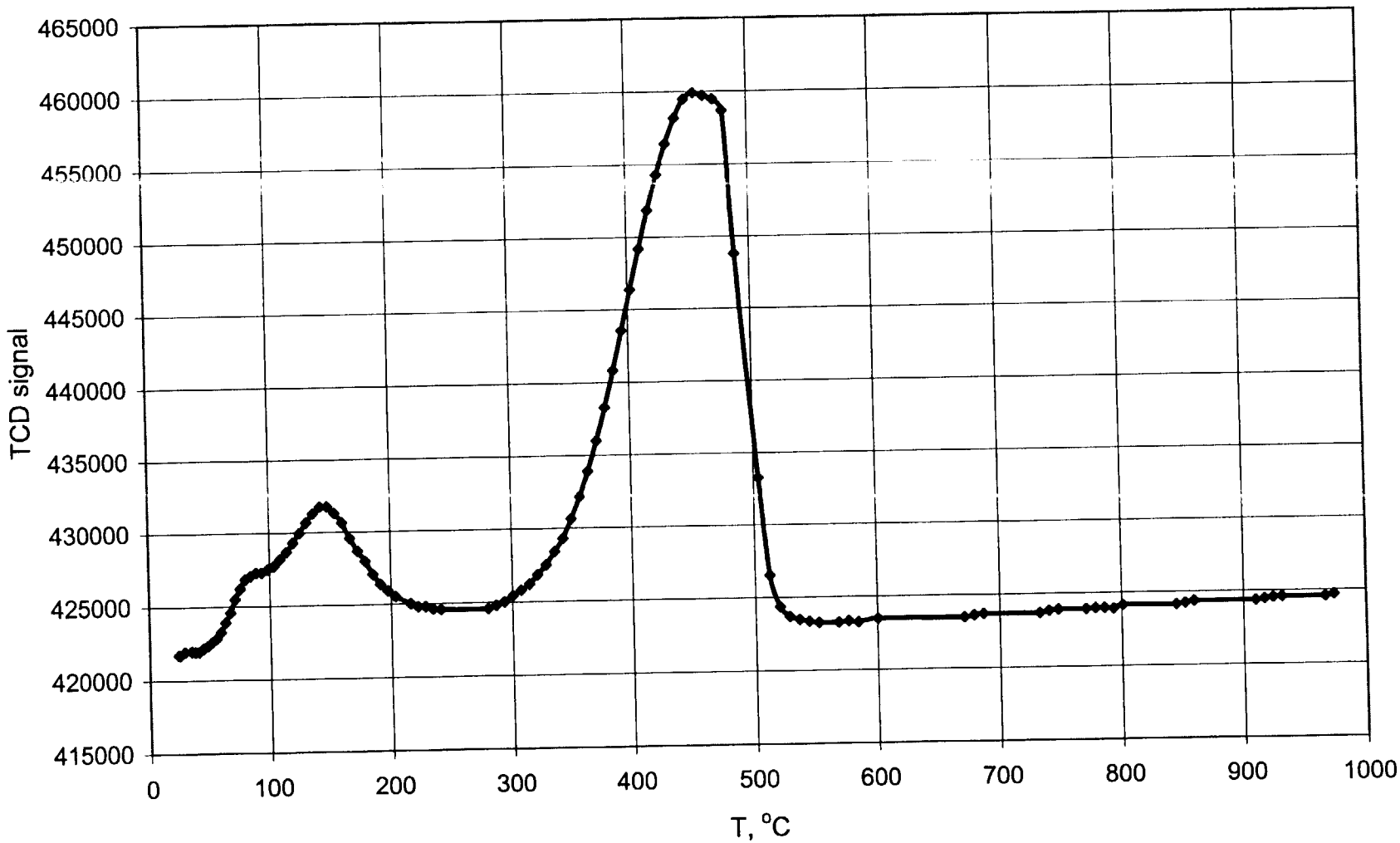

Figure 22. TPR of NASA Catalyst Sn EH only (011019/1) with 6.69 % H2 in Ar. Catalyst mass = 0.0478 g.

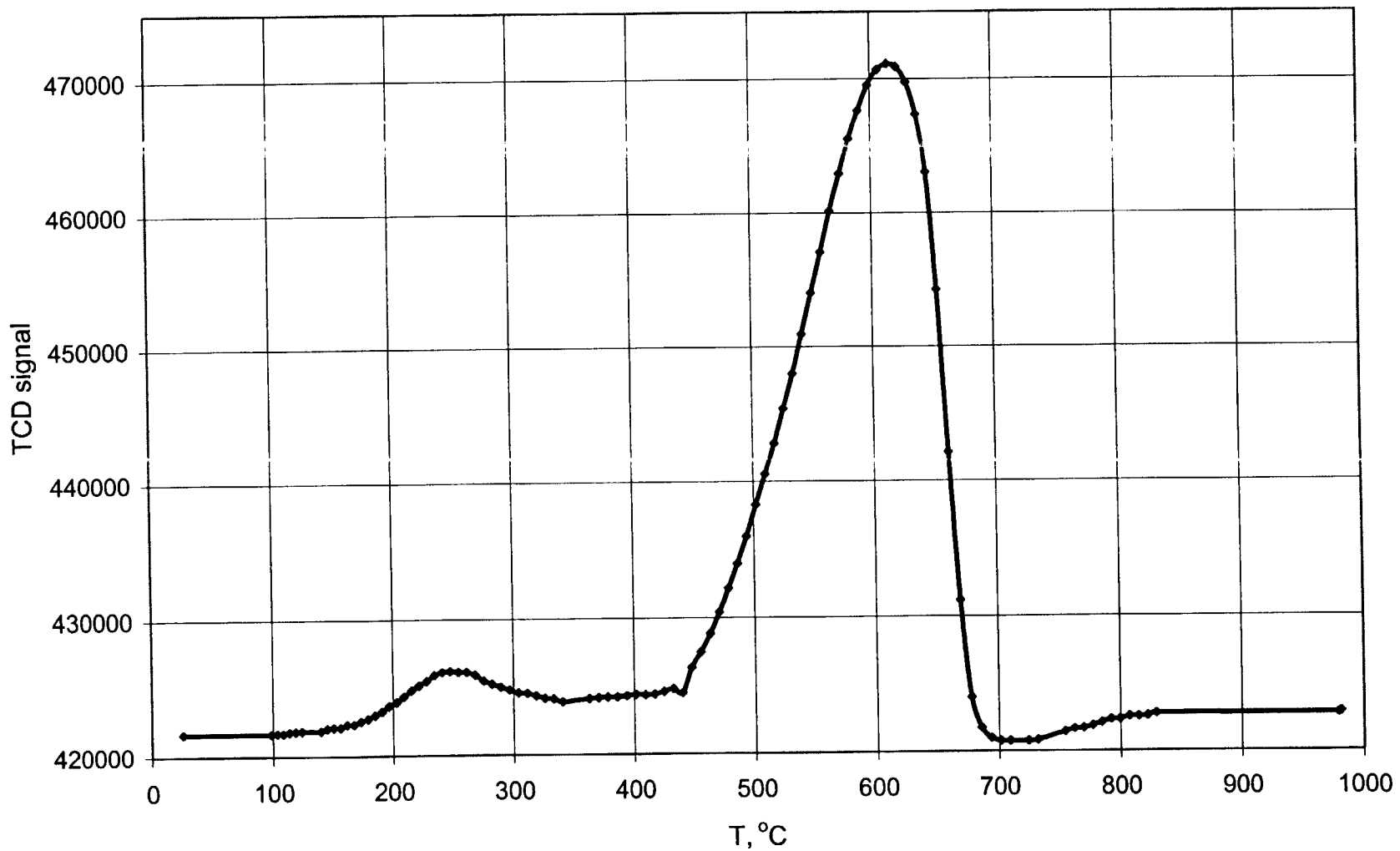

Figure 23. TPR of NASA Catalyst Sn/Ce (011019/2) with 6.69 % H_2 in Ar.Catalyst mass =0.049 g.

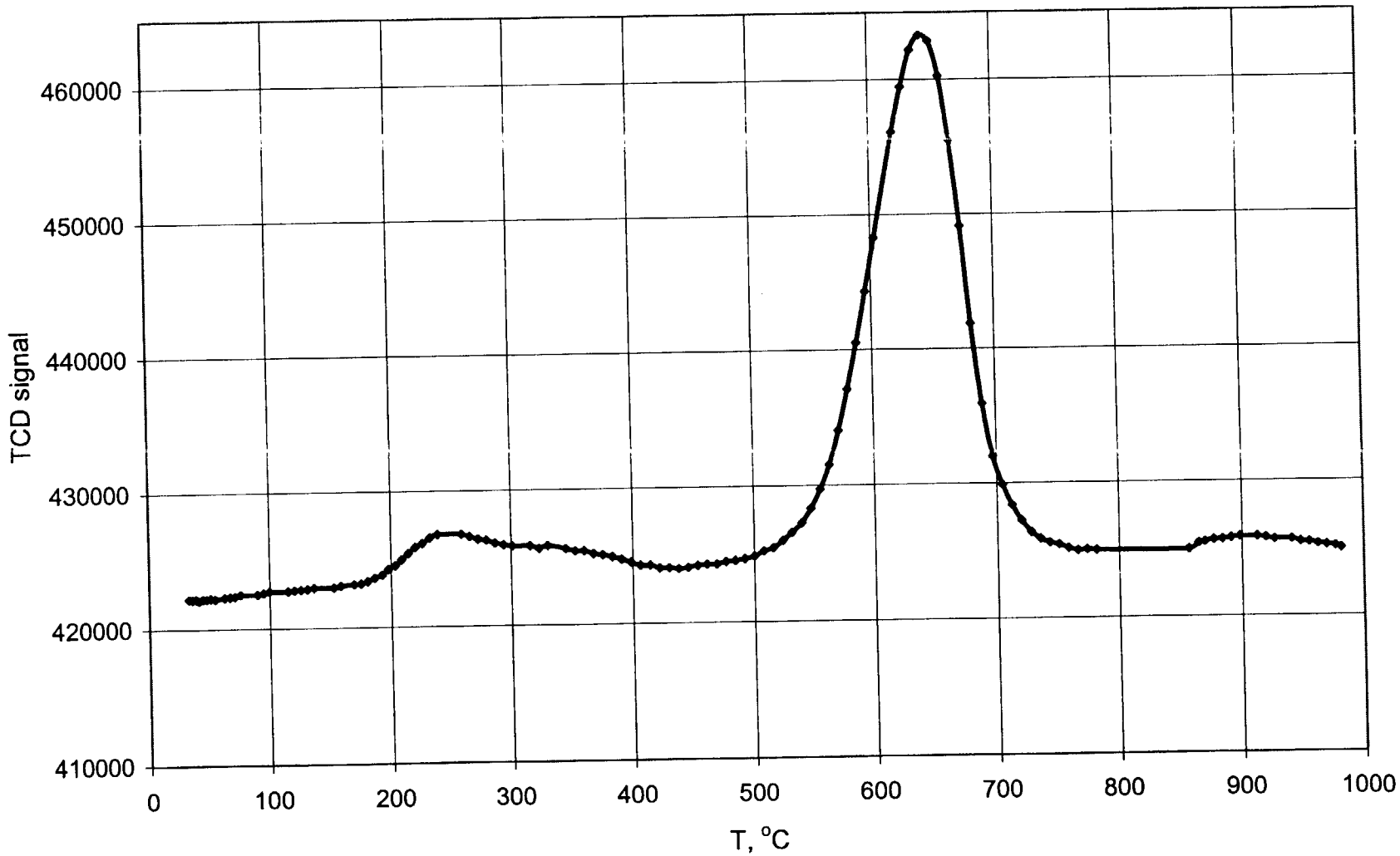

Figure 24. TPR of NASA Catalyst Sn/Ce/Zr (011019/3) with 6.69 % H_2 in Ar. Catalyst mass = 0.0418 g.

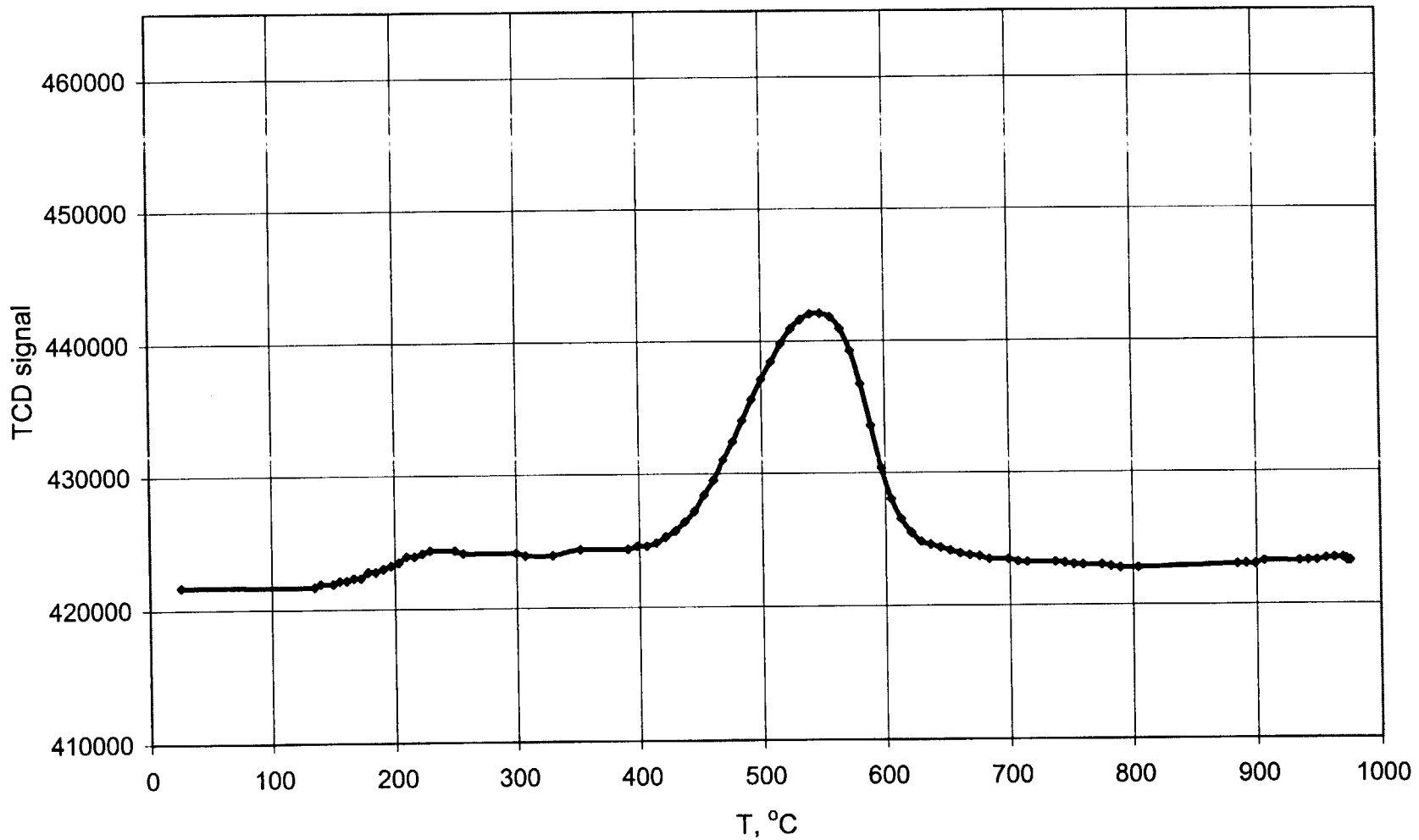

Figure 25. TPR of NASA Catalyst Sn/Ce/Zr/Al (011019/4) with 6.69 % H2 in Ar (.0452 g cat.).

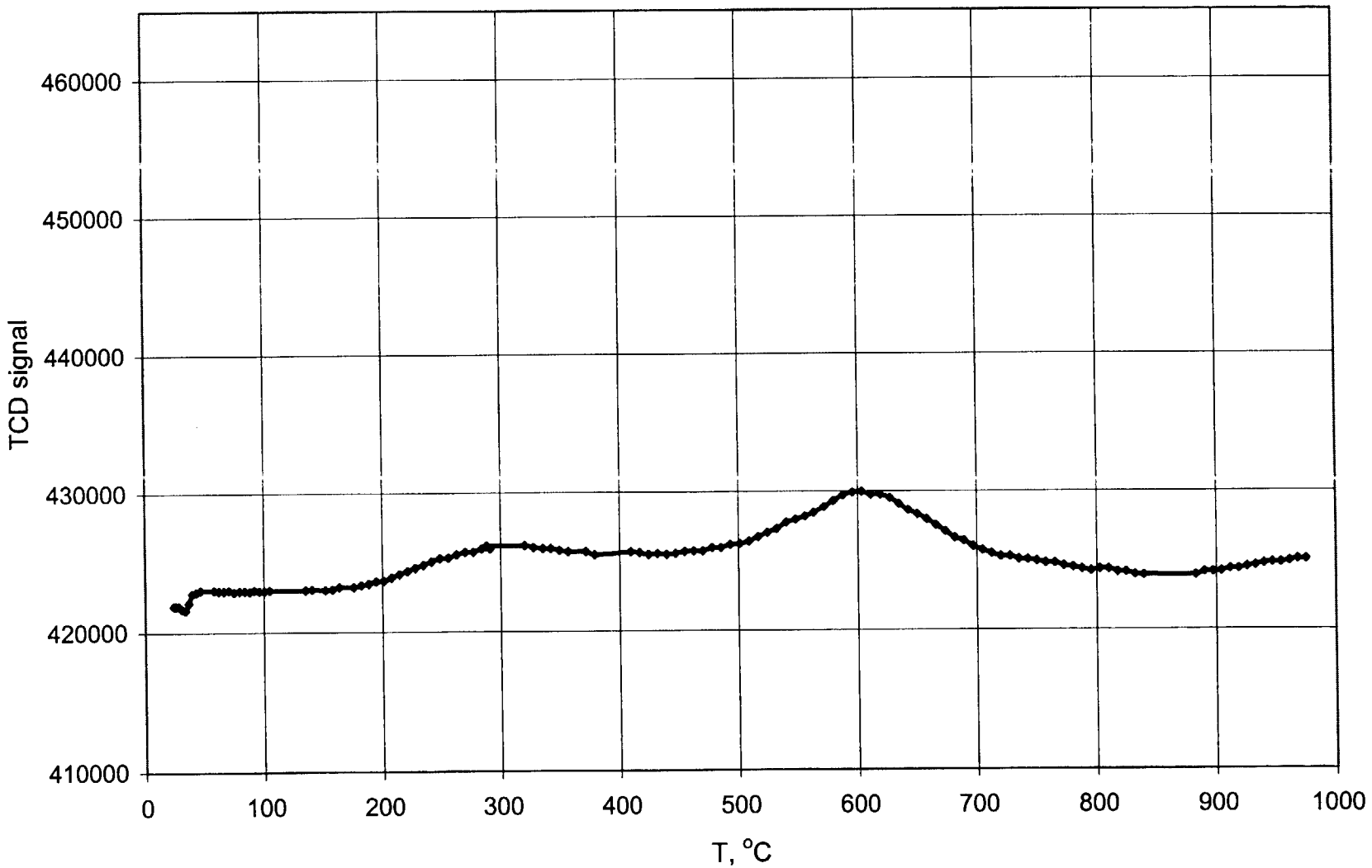

Figure 26. TPR of NASA Catalyst Sn/Zr (011019/5) with 6.69 % H_2 in Ar. Catalyst mass = 0.0454 g.

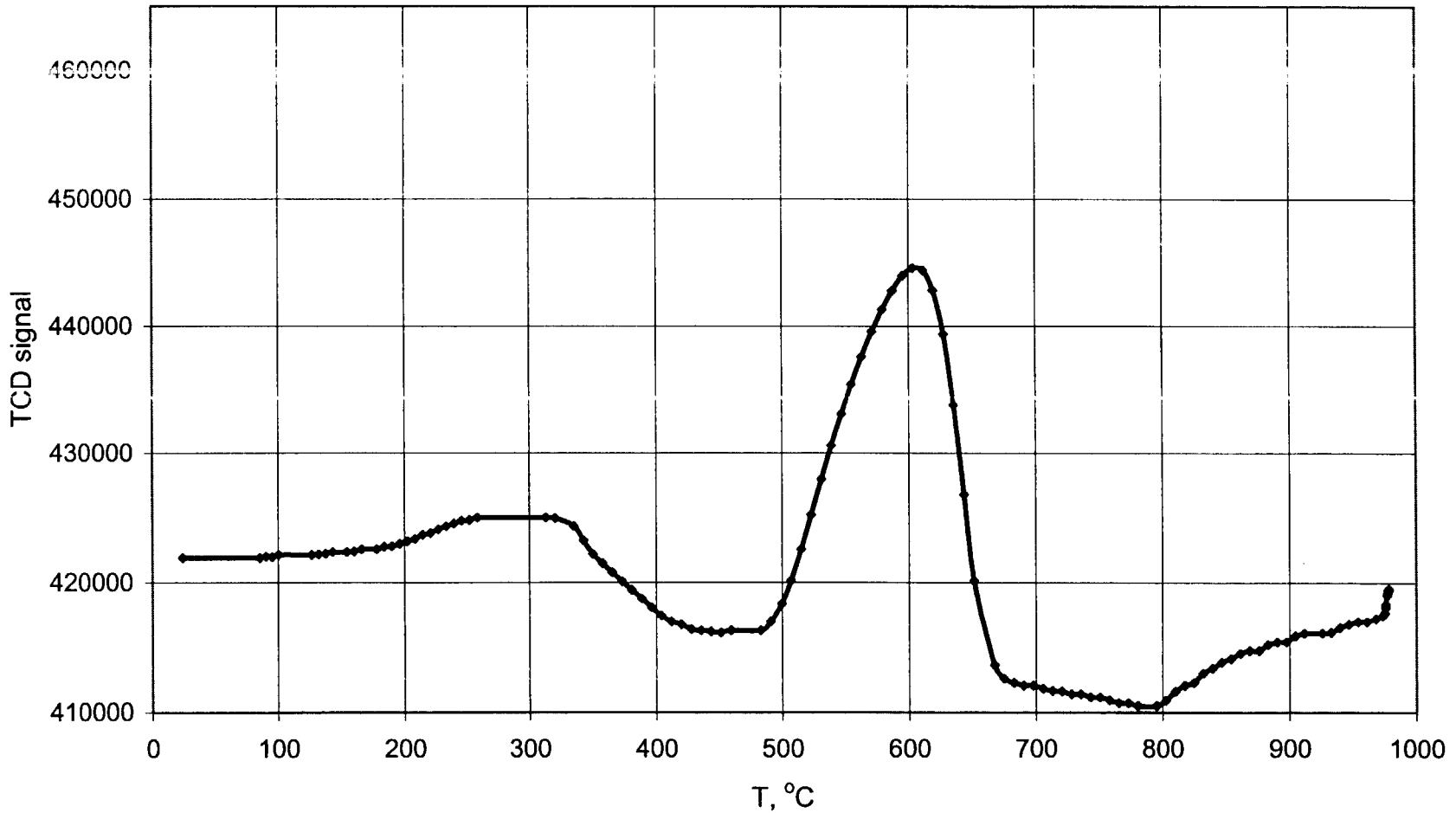

Figure 27. TPD of 15 % Pt/SnO_2 Catalyst. Effect of Pre-treatment

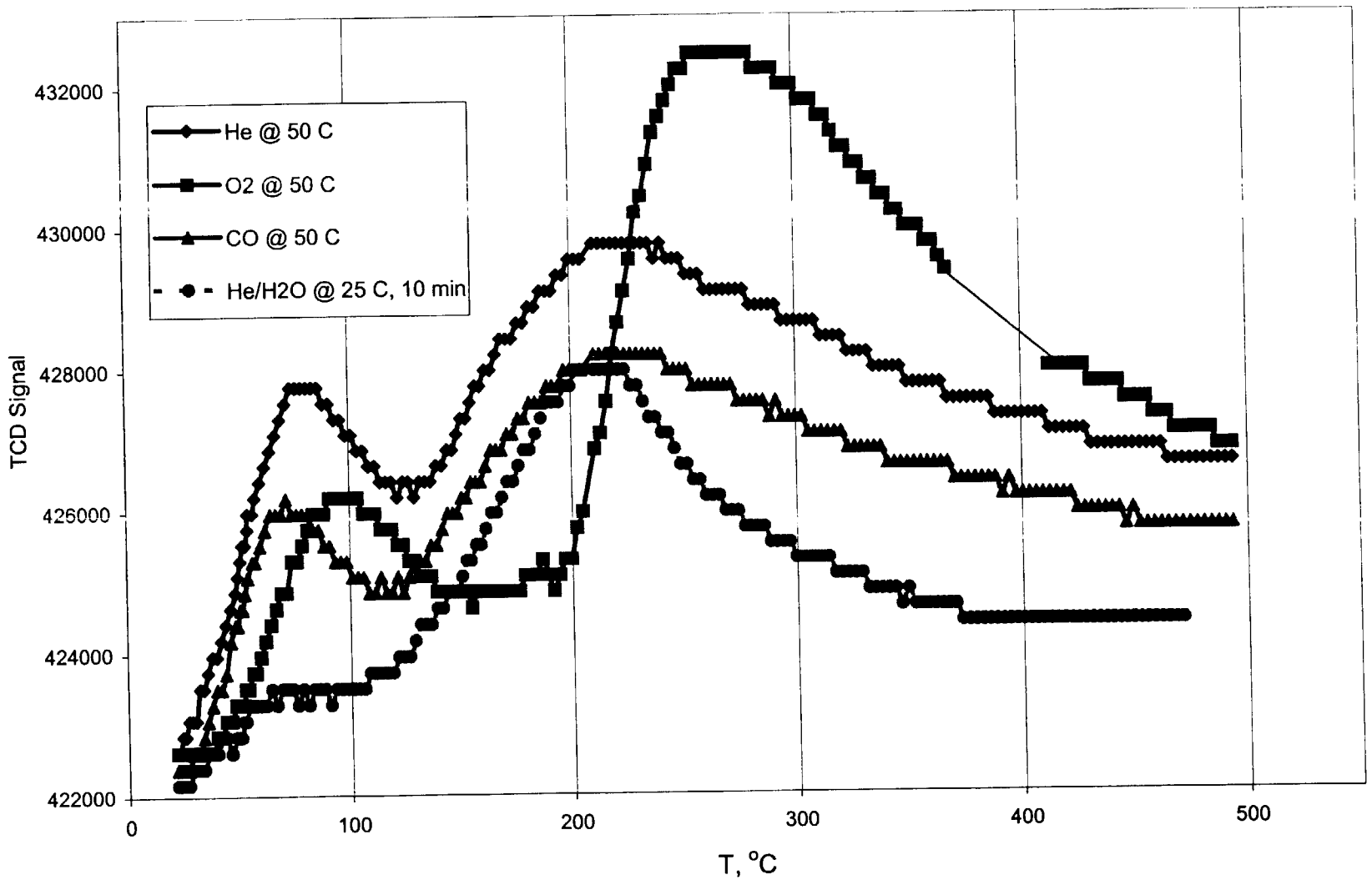

Figure 28. TPD of 15% Pt/SnO2 Catalyst After Pre-treatment with 10.1 % CO in He. Effect of Pre-treatment Temperature

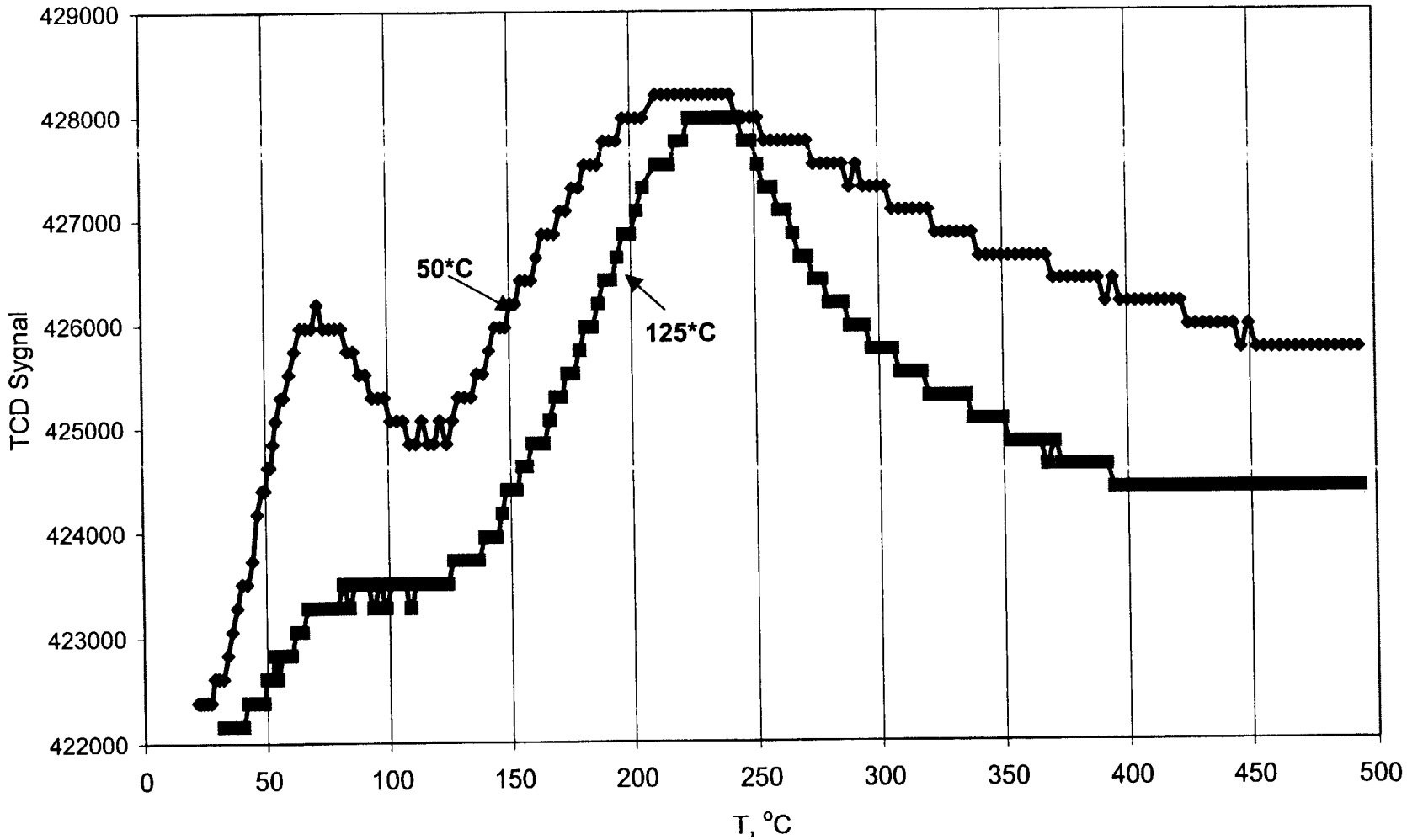

Figure 29. TPD of re-oxidized 15 % Pt/SnO_2 catalyst (NTPD007B)

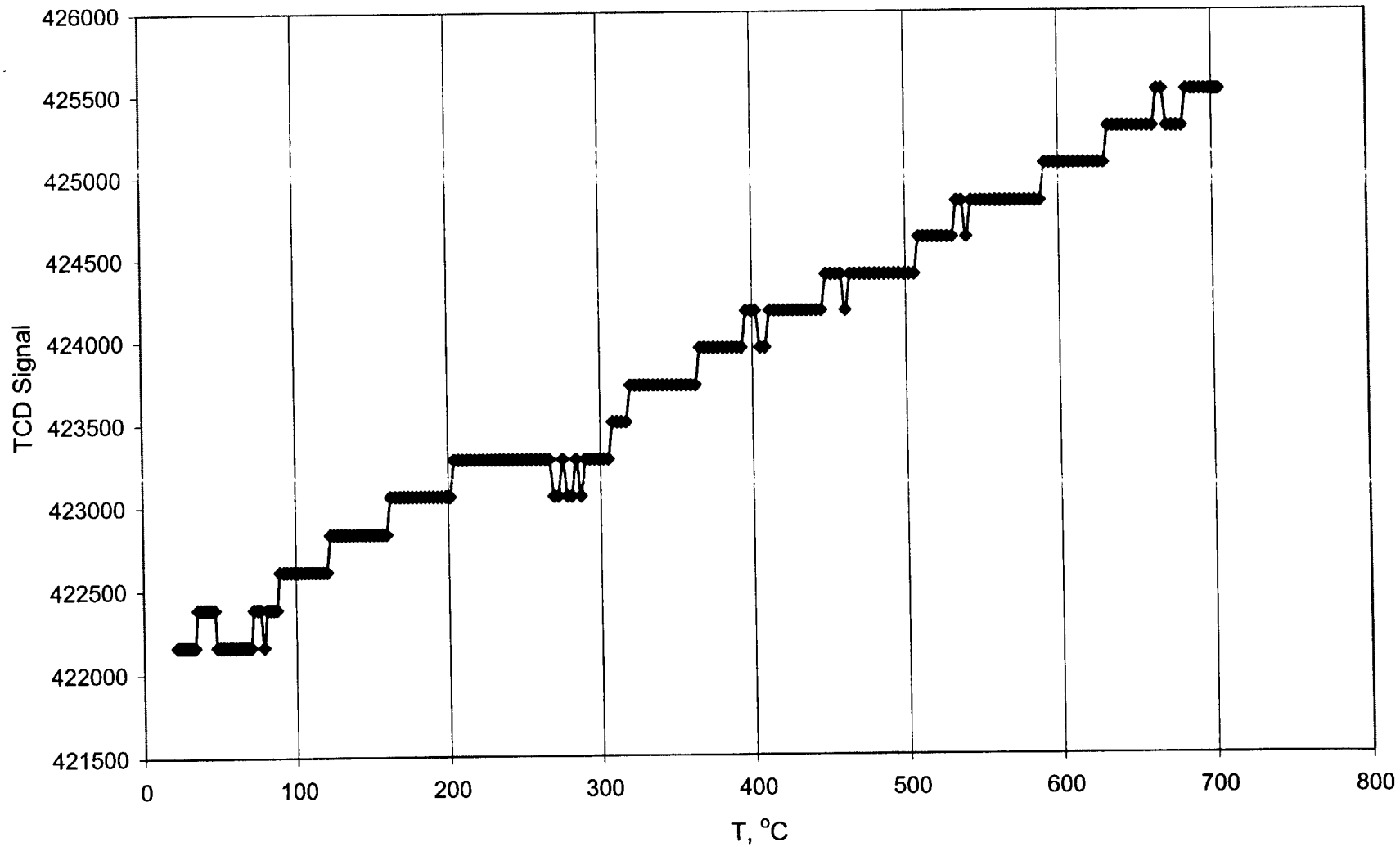

Figure 30. Species evolved and TCD peak areas on fresh 15% Pt/SnO_2 catalyst during injection of 0.993-ml doses of 10.1% CO in He at 50 ^{O}C, with He as carrier (NNTPD001A).

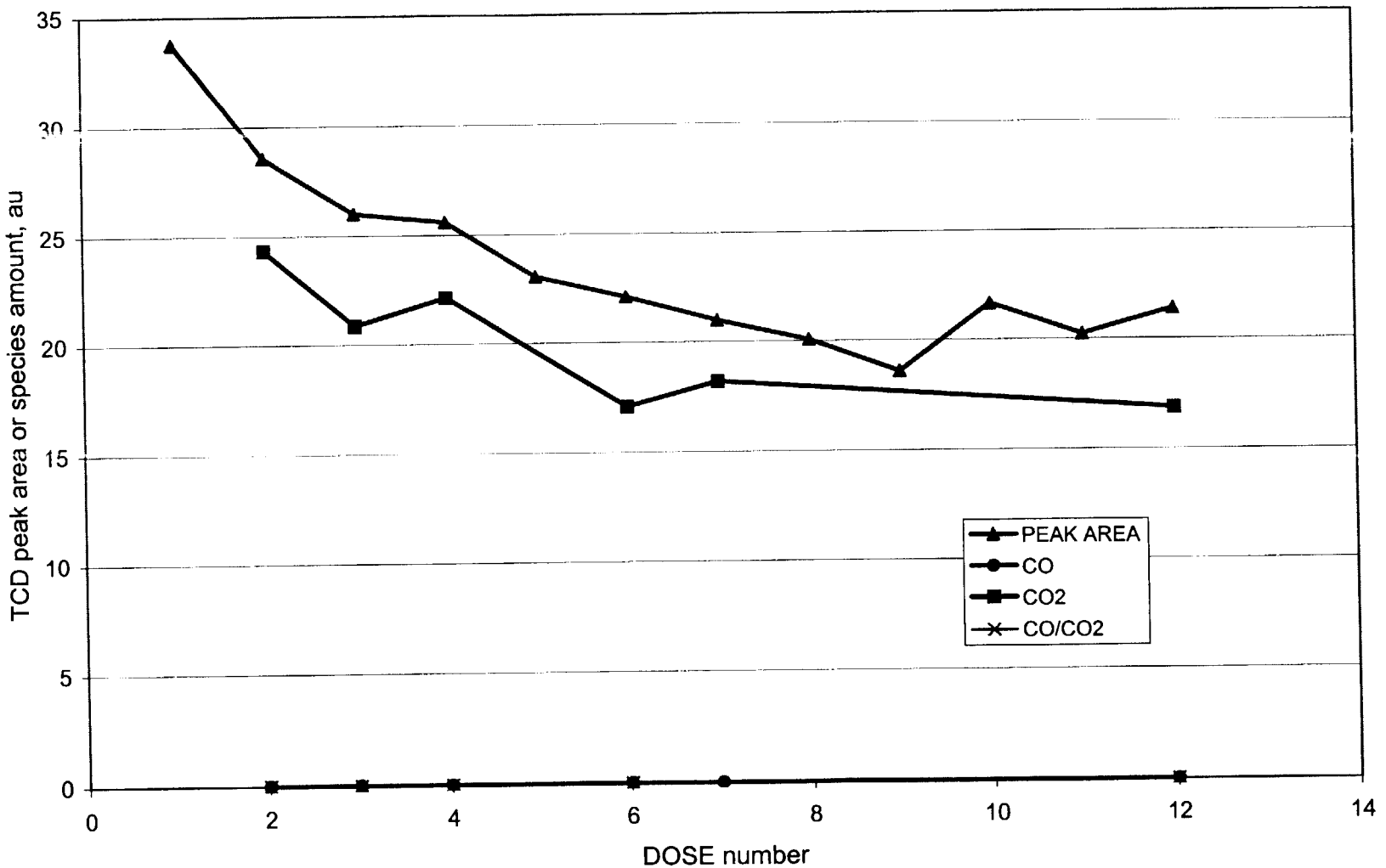

Figure 31. TPD of fresh 15 % Pt/SnO_2 catalyst, after CO injections at 50 °C, with He as carrier (NNTPD01B).

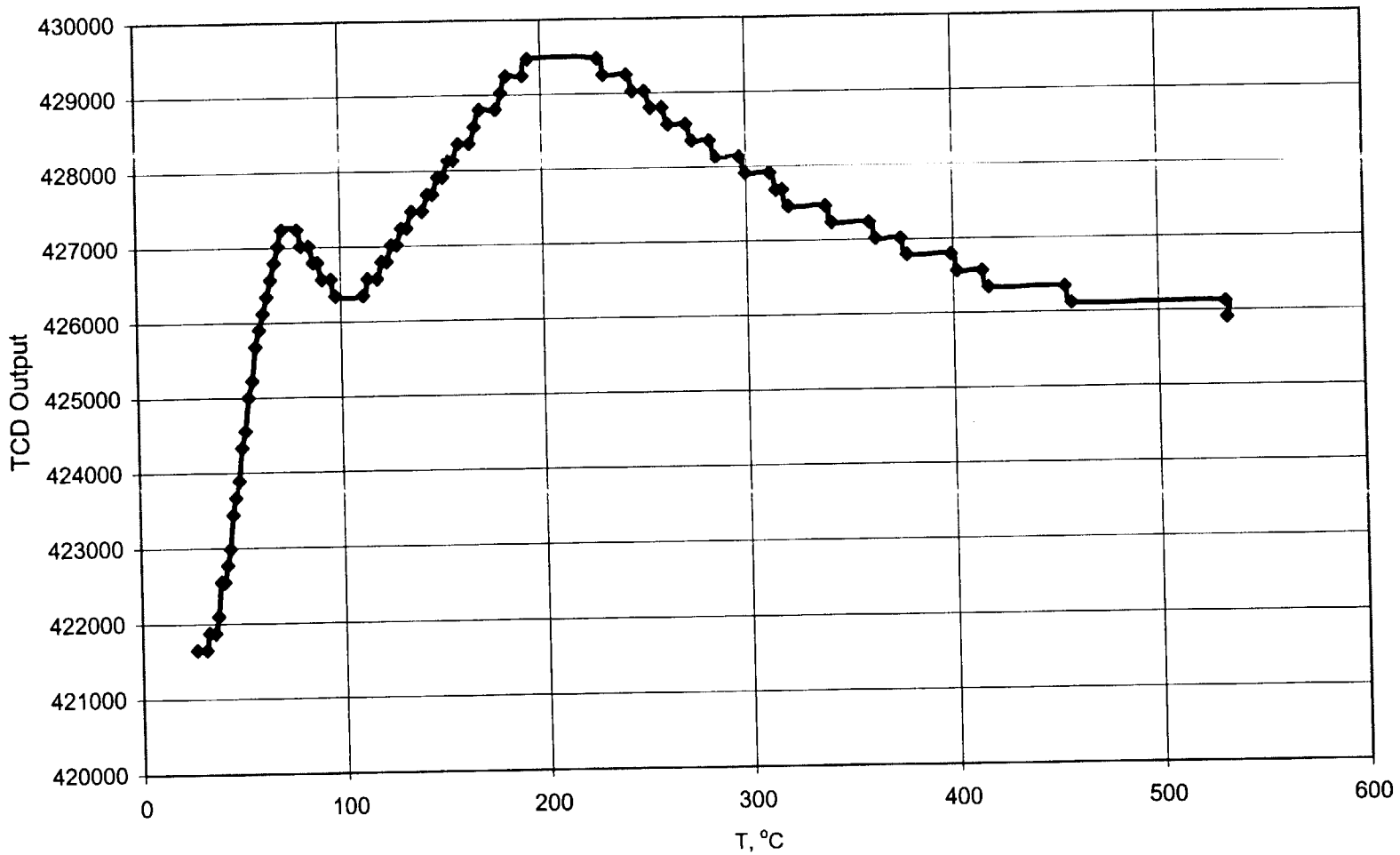

Figure 32. Species evolved during TPD of fresh 15 % Pt/SnO_2 catalyst after CO injections under dry He (NNTPD01B)

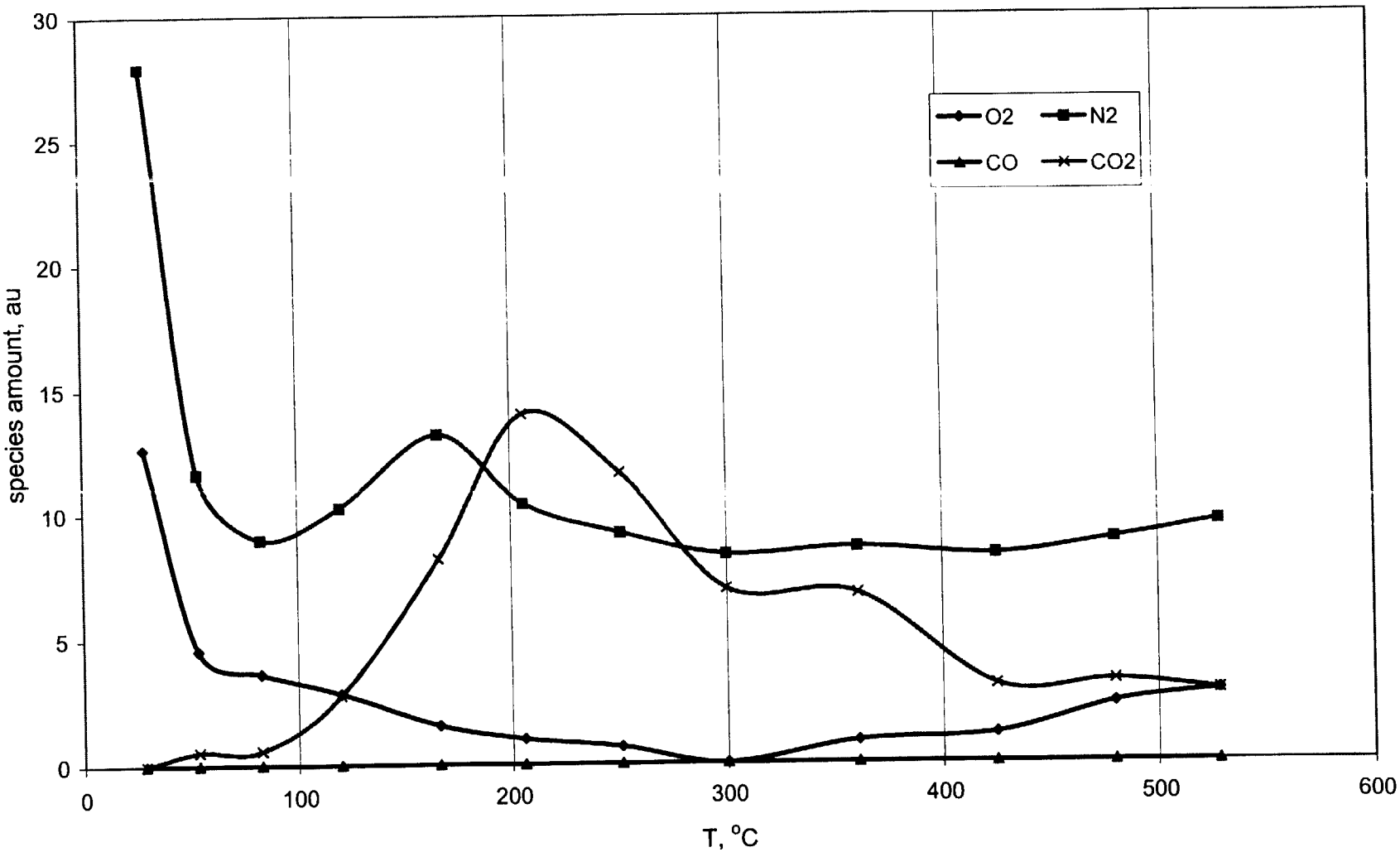

Figure 33. Species evolved and TCD peak areas on 15 % Pt/SnO_2 catalyst reoxidized after CO sorption and TPD to 530 °C, during 0.993-ml doses of 10.1% CO in He with He as carrier. (NNTPD01G)

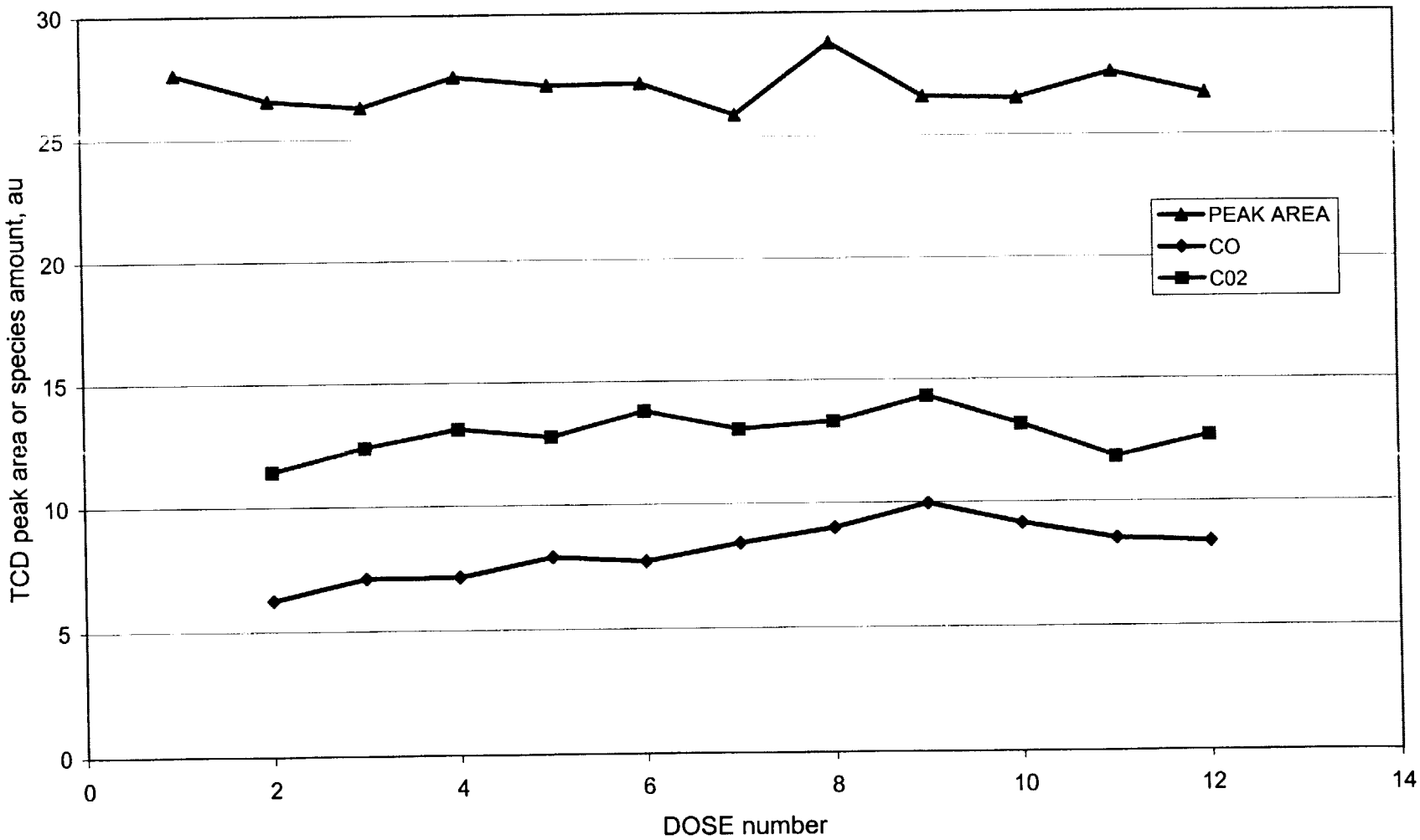

Figure 34. TPD of fresh 15 % Pt/SnO_2 catalyst after CO injections at 50 °C, with (He+3.6% O_2) as carrier (NNTPD02C).

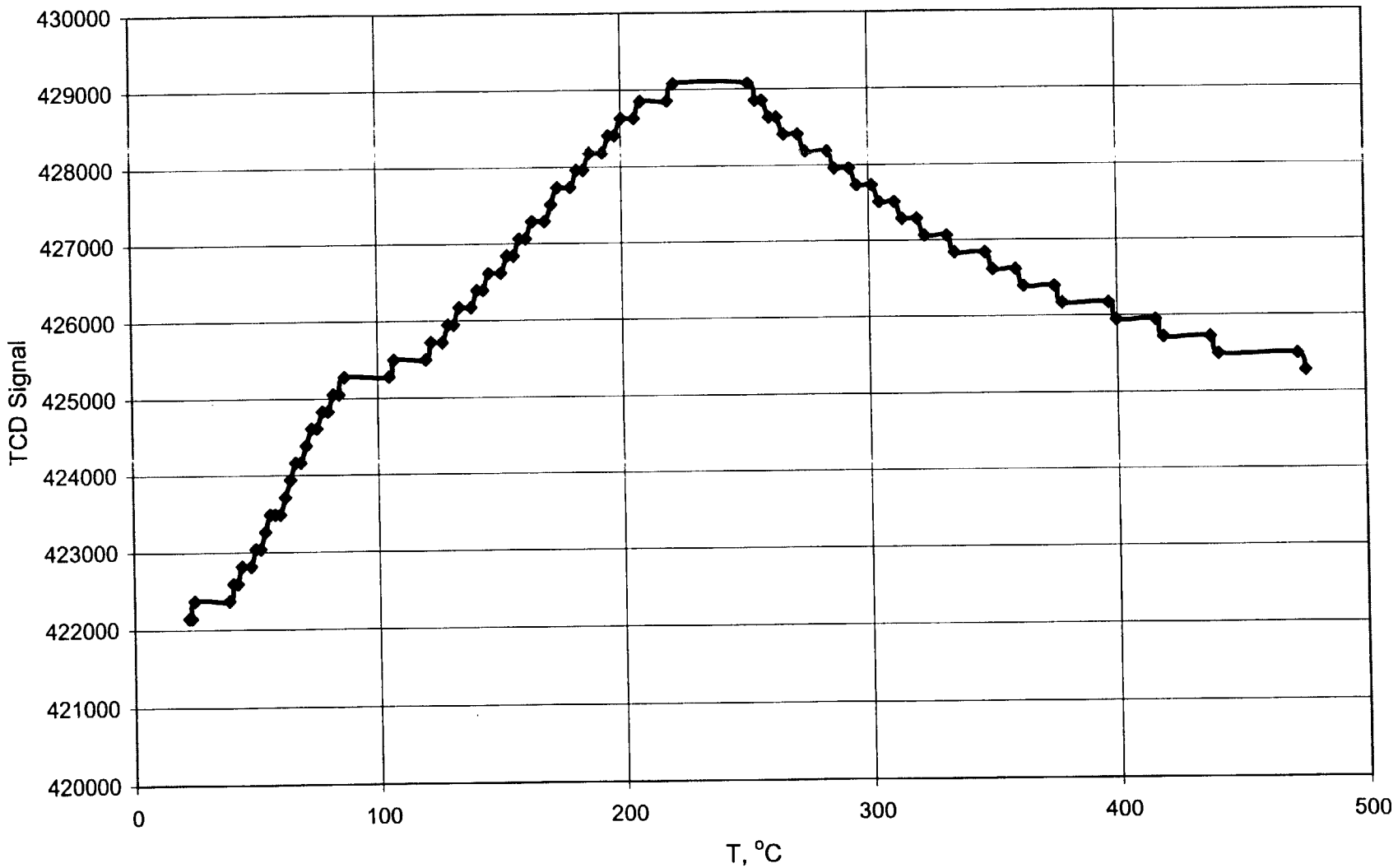

Figure 35. Species evolution during TPD of 15 % Pt/SnO_2 catalyst after CO injections at 50 °C with He+3.96% O_2 as carrier (NNTPD02C)

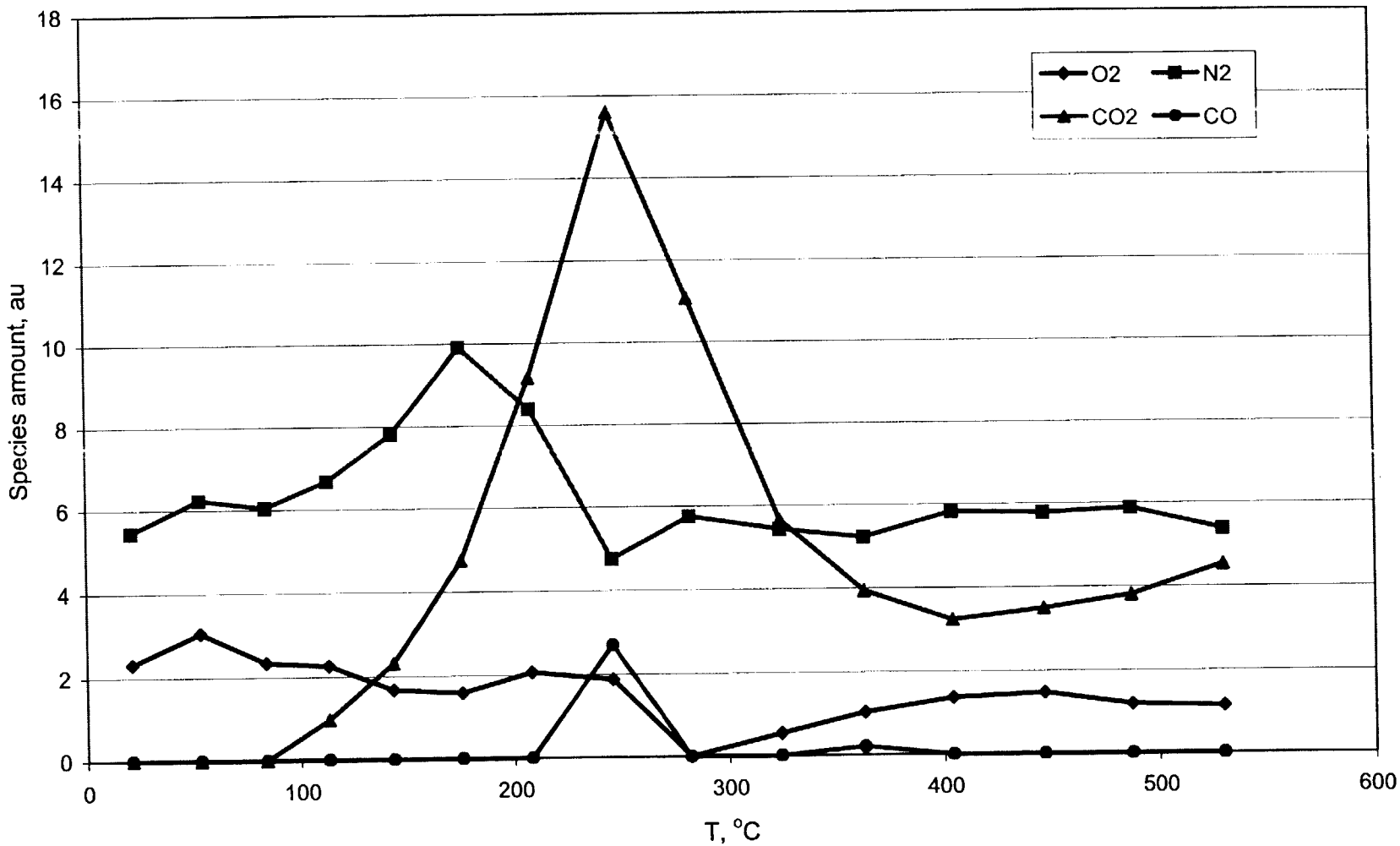

Figure 36. Species evolved and TCD peak areas on fresh 15 % Pt/SnO_2 catalyst during injection of 0.993-ml doses of 10.1% CO in He at 50 °C, with (He + 3.96% O2) as carrier (NNTPD02A).

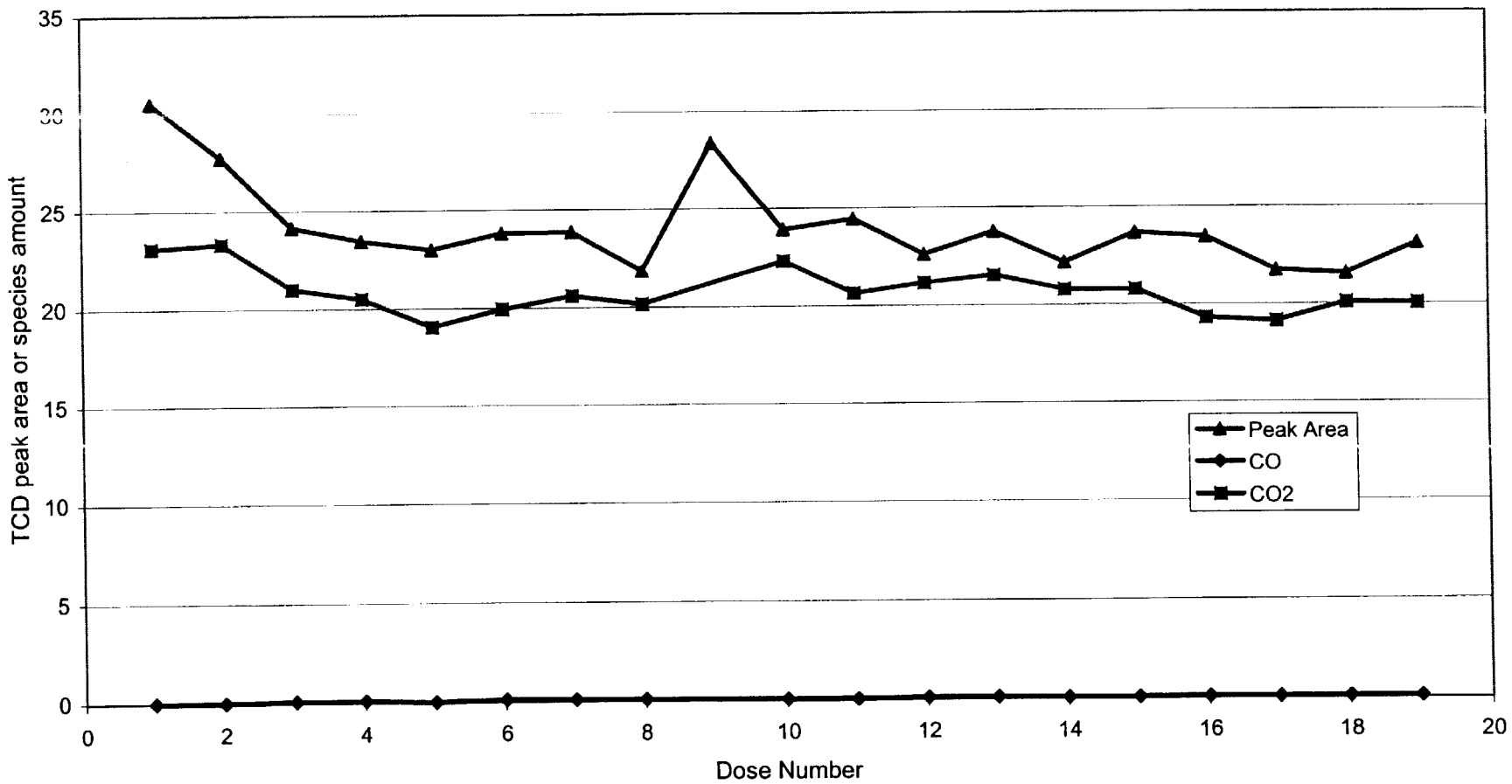

Figure 37. Species evolved and TCD peak areas during redosing with CO at 50 °C after TPD to 530 °C under He + 3.6 % O_2 . Dose volm.=0.993 ml (NNTPD02D).

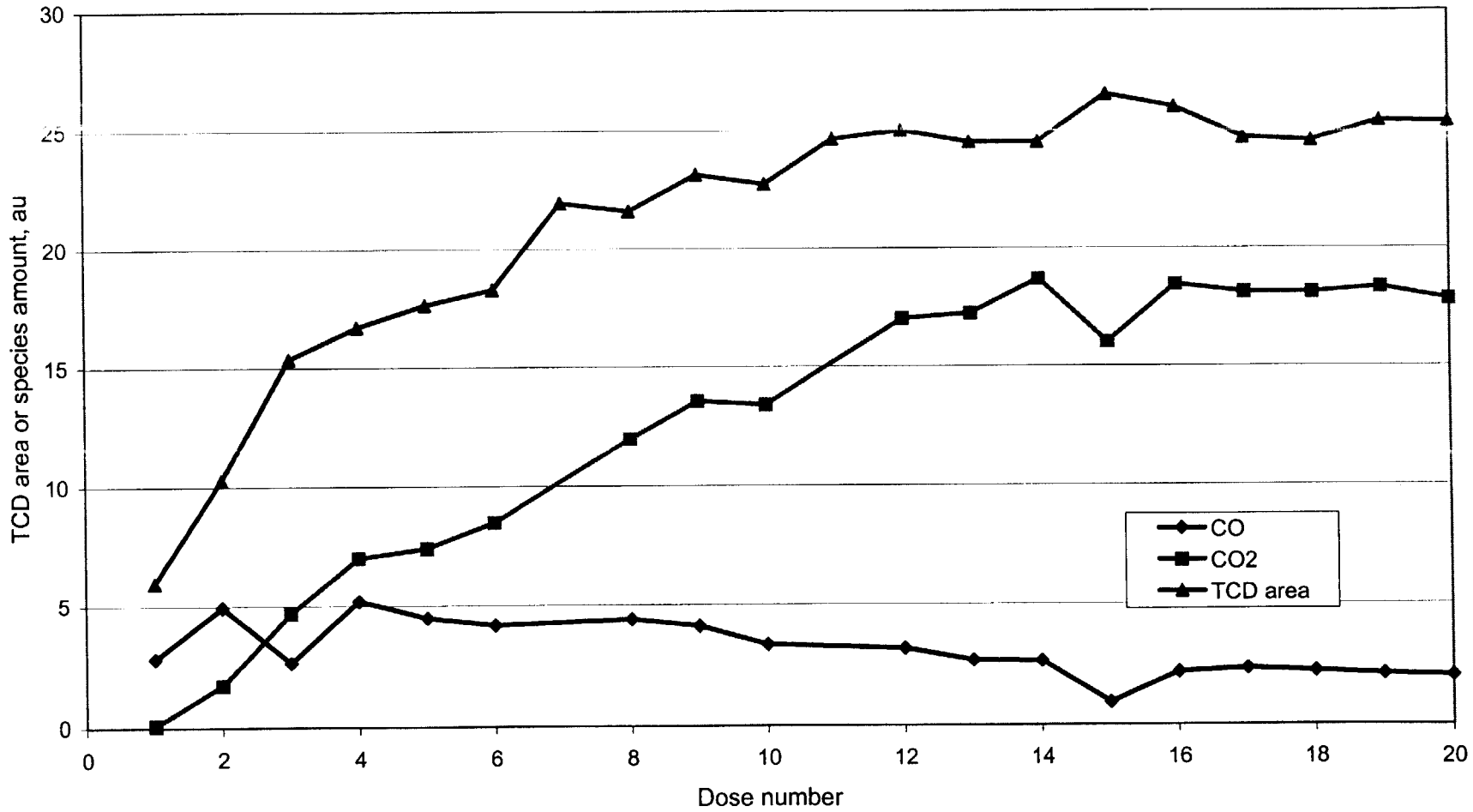

Figure 38. Species evolved and TCD peak areas on fresh 15 % Pt/SnO_2 catalyst during injection of 0.993-ml doses of 10.1% CO in He at 50 °C, with (He + 2.8% H_2O) as carrier (NNTPD02A).

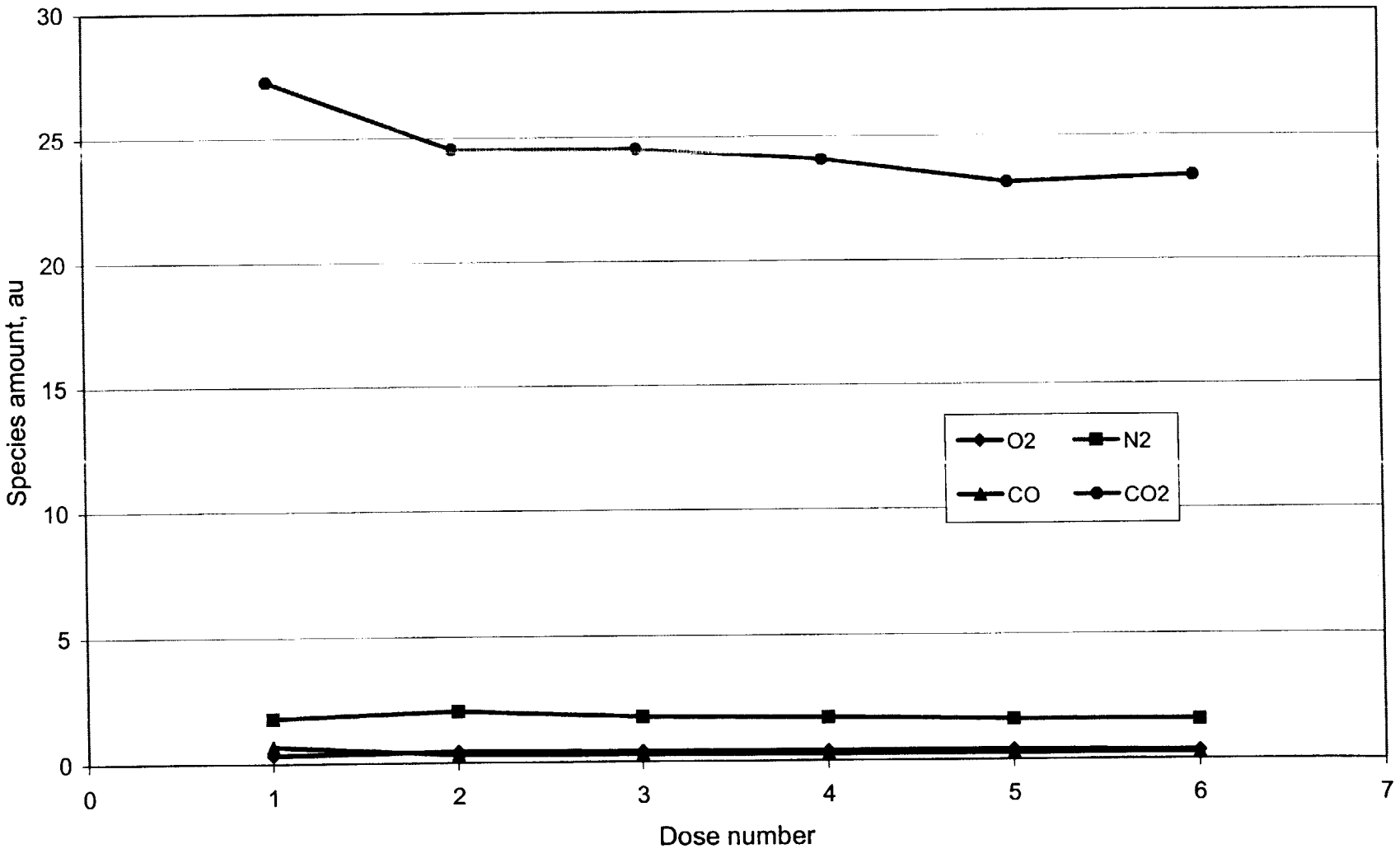

Figure 39. TPD of fresh 15 % Pt/SnO_2 catalyst after CO injections at 50°C with (He+2.8 % H_2O) as carrier

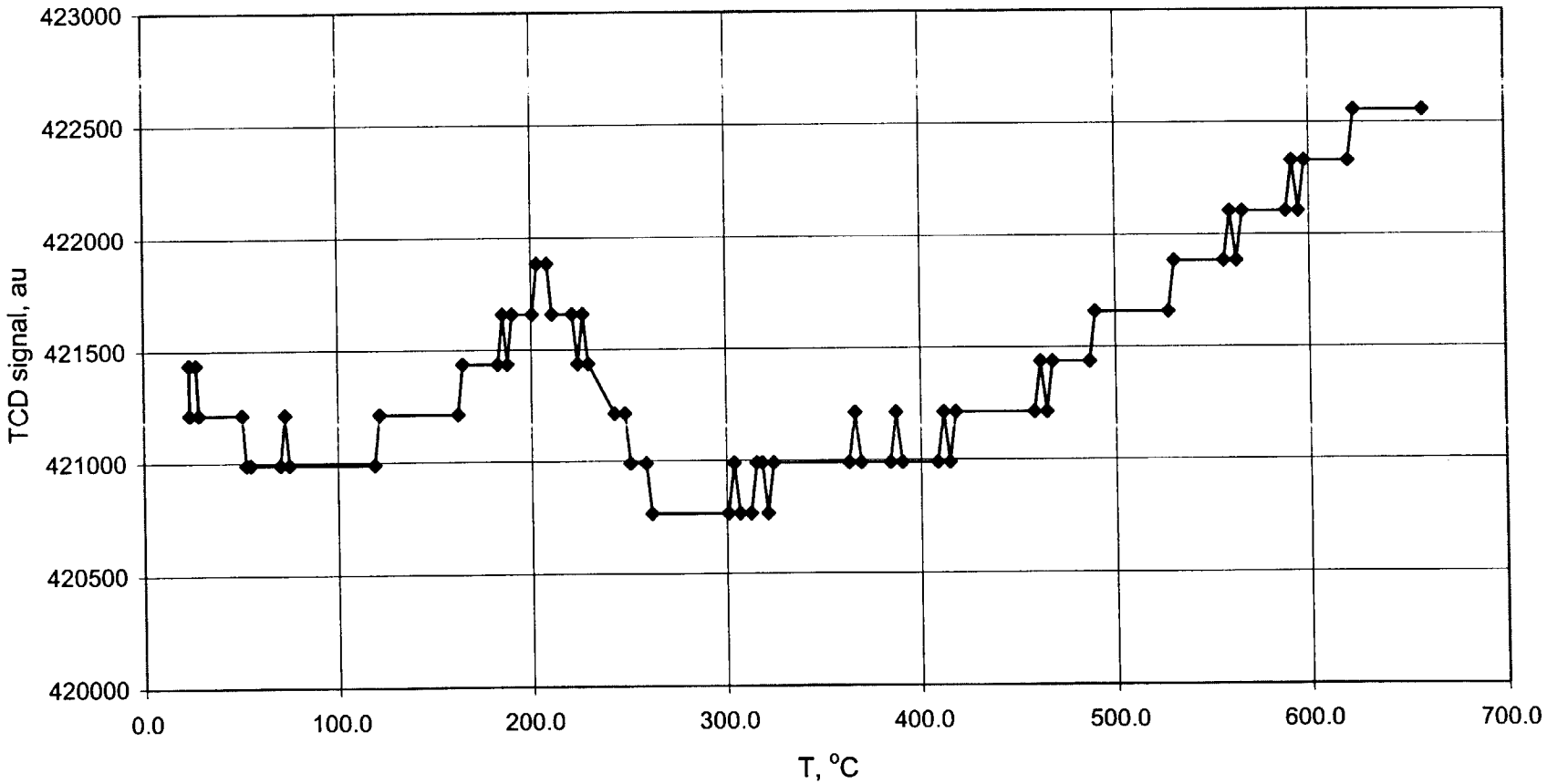

Figure 40. Species evolved during TPD of 15 % Pt/SnO_2 catalyst after CO injections at 50 °C, with (He+2.8% H_2O) as carrier

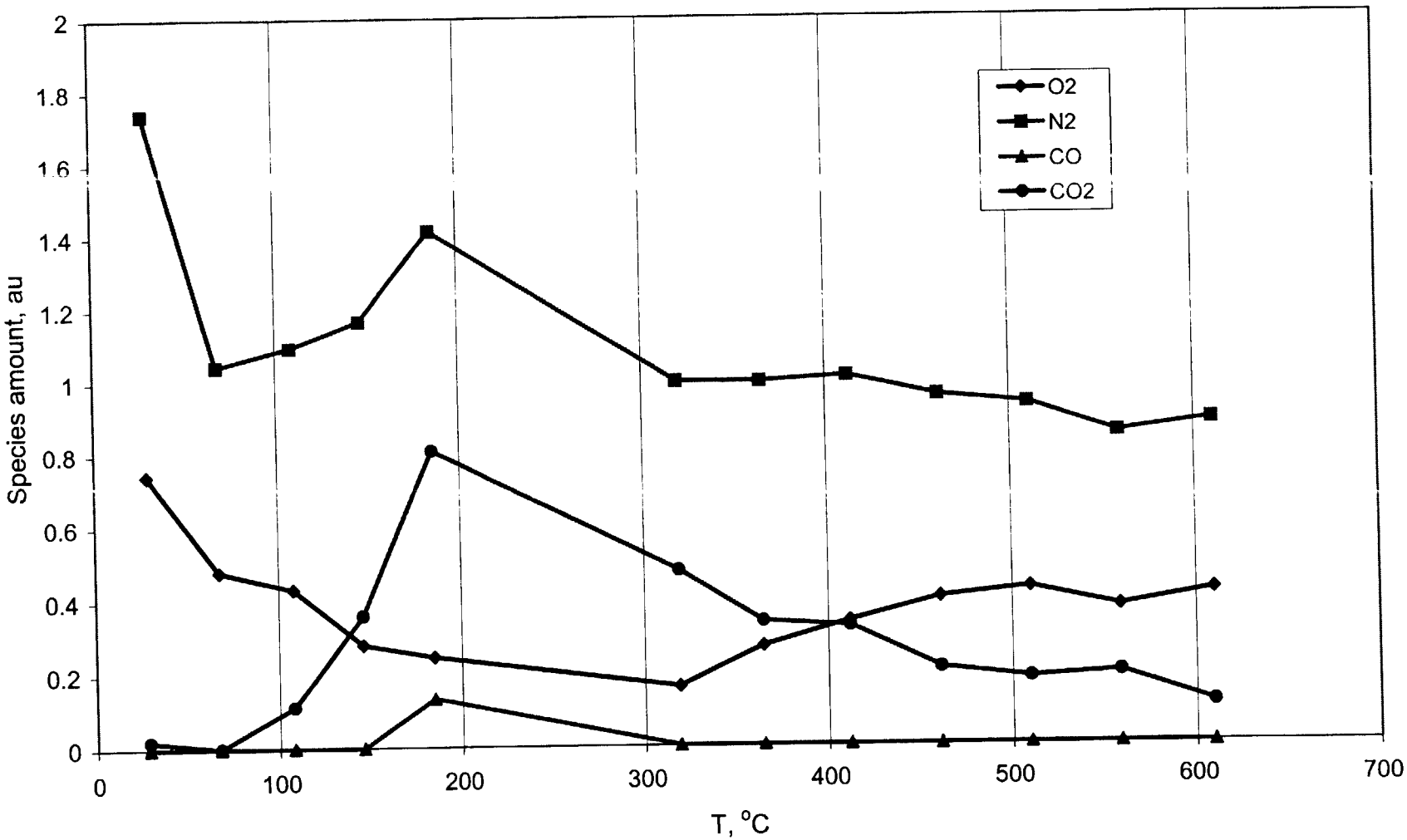

REFERENCES

1. **Herz, R. K.,** *in* "Low Temperature CO-Oxidation Catalysts for Long-Life CO2 Lasers", NASA Conf. Publ. 3076, D. R. Schryer and G. B. Hoflund, Eds., pp. 21-40, National Information Service, Springfield, VA, 1990.

2. **Schryer. D. R., Upchurch, B. T., Hess, R. V., Wood, G. M., Sydney, B. D., Miller, I. M., Brown, K. G., Van Norman, J. D., Schryer, J., Brown, D. R., Hoflund, G. B., and Herz, R. K.,** *in* "Low Temperature CO-Oxidation Catalysts for Long-Life CO2 Lasers", NASA Conf. Publ. 3076, D. R. Schryer and G. B. Hoflund, Eds., pp. 41-53, National Information Service, Springfield, VA, 1990.

3. **Upchurch, B. T., Kielin, E. J., and Miller, I. M.,** *in* "Low Temperature CO-Oxidation Catalysts for Long-Life CO2 Lasers", NASA Conf. Publ. 3076, D. R. Schryer and G. B. Hoflund, Eds., pp. 69-90, National Information Service, Springfield, VA, 1990.

4. **Van Norman, J. D., Brown, K. G., Schryer, J., Schryer. D. R., Upchurch, B. T., Sydney, B. D.,** *in* "Low Temperature CO-Oxidation Catalysts for Long-Life CO2 Lasers", NASA Conf. Publ. 3076, D. R. Schryer and G. B. Hoflund, Eds., pp. 181-191, National Information Service, Springfield, VA, 1990.

5. **Upchurch, B. T., Wood, G. M., Schryer. D. R., Hess, R. V., Miller, I. M., Kielin, E. J.,** *in* "Low Temperature CO-Oxidation Catalysts for Long-Life CO2 Lasers", NASA Conf. Publ. 3076, D. R. Schryer and G. B. Hoflund, Eds., pp. 41-53, National Information Service, Springfield, VA, 1990.

6. **Gardner, S. D., Hoflund, G. B., Schryer. D. R., Upchurch, B. T.,** *in* "Low Temperature CO-Oxidation Catalysts for Long-Life CO_2 Lasers", NASA Conf. Publ. 3076, D. R. Schryer and G. B. Hoflund, Eds., pp. 217-229, National Information Service, Springfield, VA, 1990.

7. **Keiser, J. T. and Upchurch, B. T.,** *in* "Low Temperature CO-Oxidation Catalysts for Long-Life CO_2 Lasers", NASA Conf. Publ. 3076, D. R. Schryer and G. B. Hoflund, Eds., pp. 313-320, National Information Service, Springfield, VA, 1990.

8. **Brown, K. G., Ohorodnik, S. K., Van Norman, J. D., Schryer, J., Upchurch, B. T., Schryer. D. R.,** *in* "Low Temperature CO-Oxidation Catalysts for Long-Life CO2 Lasers", NASA Conf. Publ. 3076, D. R. Schryer and G. B. Hoflund, Eds., pp. 41-53, National Information Service, Springfield, VA, 1990.

9. **Schryer. D. R., Upchurch, B. T.,** "Low Temperature Oxidation Catalysts: A Mechanistic Overview", unpublished private communication.

10. **Haruta, M., Tsubota, S., Kobayashi, T., Kageyama, H., Genet, M. J., and Delmon, B.,** *Journal if Catalysis* 144, 175-192, 1993.

11. **Gardner, S. D., Hoflund, G. B., Schryer. D. R., Schryer, J., Upchurch, B. T., and Brown, D. R.,** *in* "Low Temperature CO-Oxidation Catalysts for Long-Life CO_2 Lasers", NASA Conf.

Publ. 3076, D. R. Schryer and G. B. Hoflund, Eds., pp. 123-137, National Information Service, Springfield, VA, 1990.

12. **Jin, T., Okuhara, T., Mains, G. J., and White, J. M.,** *J. Phys. Chem. B* 91, 3310-3315, 1997.

13. **Martinez-Arias, A., Coronado, J. M., Cataluna, R., Conesa, J. C., and Soria, J.,** *J. Phys. Chem. B* 122, 4357-4365, 1998.